Dish to digital: Amazing growth in military radar antenna technology

A. K. Singh

Abstract | Radar is a vulnerable technology. Today's military radar systems perform a variety of tasks which were not possible by the radar systems developed more than 6 decades ago during world war II. There has been continuous efforts towards upgrading the radar system and associated technologies with drastic improvement in the performance. Almost every current radar innovation owes its existence to the advances made in the antenna technology to achieve a very high efficiency and ultra low side lobes with computer intensive design. There has been a phenomenal growth in Military radar antenna technology over the last few decades. The present paper deals with the design and development of various types of antenna systems for different military radar applications & growth in the technology over last three decades in the country, particularly, at LRDE, a radar laboratory of Defence Research & Development Organization.

1. Introduction

Today's military radar systems perform a variety of tasks that were not possible by the radar systems developed during world war II. There have been continuous efforts towards upgrading the radar systems and associated technologies with drastic improvement in the performance. Almost every current radar innovation owes its existence in the advances made in the antenna technology to achieve a very high efficiency and ultra low side lobes with computer intensive design. In recent years, the antenna and radar systems have seen amazing advancements that led the capabilities not possible few years back.

Over last three decades, Electronics and Radar Development Establishment (LRDE) has been concentrating in developing variety of antenna systems and associated technologies for various radars developed for military use in India. LRDE has been implementing futuristic technologies in all the antenna systems and adopted various state-of-the-art technologies to perfect the design, manufacturing and integration with Radar systems successfully. To meet the radar system requirement in terms of range, coverage and resolutions, antenna needs to generate beams of desired pattern beam shape, beam width, side lobe level and directivity with the additional ability to steer the beam in desired directions. These antennas differ in how the radiated beam is formed and how the beam is steered.

Antenna technology has gone through several changes commensurate with the evolution of complex radar systems for various military applications. Present paper gives an overview of the antenna system and related technologies developed over the years to meet the requirement of armed forces. For the sake of convenience, the development of antenna systems has been categorised in terms of how the antenna beam of the required beamwidth, side lobe level, gain and other antenna characteristics are steered to give the volumetric coverage of the entire space the radar is looking into.

Electronics and Radar Development Establishment, Defence Research and Development Organisation, C. V. Raman Nagar, Bangalore 560 093, India
singhak62@yahoo.com

1.1. *Antennas and antenna arrays*

An antenna is defined by Webster's Dictionary as "a usually metallic device (as rod or wire) for radiating or receiving radio waves". The IEEE standard definition of terms for antennas (IEEE Std 145-1983)[1,2] defines the antenna or aerial as "a means for radiating or receiving radio waves". In other words the antenna is the transitional structure between free space and a guiding device. The guiding device or transmission line may take the form of a co-axial line or waveguide, and it is used to transport the electromagnetic energy from the transmitting source to the antenna or from the antenna to the receiver. In the former case we have a transmitting antenna and in the latter case a receiving antenna. Transmit and receive antenna have the same impedance and radiation pattern at a given frequency.

There are various types of antennas[2] such as wire antennas (dipoles, loop helix etc), aperture antenna (waveguides, horn, reflectors), array antennas, lens antennas etc. Antenna is characterized by various parameters, the most important ones are the gain (directivity) and radiation pattern of the antenna. Radiation pattern of an antenna is a graphical representation, usually in the far field region, of one of the antenna parameters like amplitude, phase or polarization. In amplitude pattern, a main (major) lobe is defined as the radiation lobe containing the direction of maximum radiation. A Side lobe is defined as radiation lobe in any direction other than the major lobe. Amplitude level of side lobe relative to the main lobe is called side lobe level.

To enhance the directivity of the antenna and to have the desired radiation pattern, number of antennas are grouped to form an array. An antenna array is an assembly of antennas in an electrical and geometrical configuration where elements are identical in most of the cases. Based on the element used, these would include slotted arrays, microstrip arrays, or dipole arrays. The array can be classified as linear array, curvilinear arrays, planar arrays and conformal arrays. In linear arrays elements can be distributed in a straight line (equally or unequally spaced) with elements having equal or unequal amplitude and phase distribution. In curvilinear arrays elements are distributed along a given curve. In planar arrays, elements are distributed over a plane, quite often may be regarded as a linear array of elements which are themselves linear arrays along the transverse direction. In conformal arrays elements are distributed over a given surface.

As described in[2], the antenna engineering is a vigorous discipline and this technology has been an indispensible partner of the radar and communication revolution over the last 70 years or more. Many of the major advances in antenna technology that have been completed in the 1970s through the early 1990s are captured in a set of review articles in[3].

1.2. *Requirements for radar antennas*

The radar antenna is a distinctive and important part of any radar. It serves the following functions[4]:

(i) Act as the transducer between propagation in space and guided wave propagation in the transmission lines
(ii) Concentrates the radiated energy in the direction of the target (as measured by the antenna gain)
(iii) Collects the echo energy scattered back to the radar from a target. (as measured by the antenna effective aperture)
(iv) Measures the angle of arrival of the received echo signal so as to provide the location of the target in azimuth, elevation or both.
(v) Acts as a spatial filter to separate (resolve) targets in the angle (spatial) domain, and rejects undesired signals from directions other than the main beam.
(vi) Provides the desired volumetric coverage of the radar.
(vii) Usually establishes the time between radar observations of a target (revisit time).

With radar antennas, big is beautiful—within the limits of the mechanical and electrical tolerances and the constraints imposed by the physical space available on the platform that carries the antenna. The larger the antenna, the better the radar performance, the smaller can be transmitter, and the less can be the total amount of prime power needed for the radar system. The transmitting antenna gain and the receiving effective aperture are proportional to one another so that a large transmitting gain implies a large effective aperture, and vice versa.

For most of the military radar applications, antenna with a very high gain (directivity), low beam width and very low side lobe levels are the desired features. Almost all the radar antennas are directive and have some means for steering the beam in angle. Directive antennas have narrow beams, which result in accurate angular measurements and thereby allowing closely spaced targets to be resolved. Low side lobes are desired to avoid detecting large targets when they are illuminated by side lobes. Any echo received from the side lobe will not be indicated by their true angle. (The angle assigned to an echo from a side lobe will be the angle at which the main beam points at the time of detection rather than the angle of the side lobe which illuminates the target.) Low side lobes are also useful for minimizing the effect of strong jamming and interference and to reduce the large clutter echoes that can enter the antenna side lobes.

Antenna designers have a variety of directive antenna types from which to choose including

Figure 1: Height *vs*. range coverage diagram.

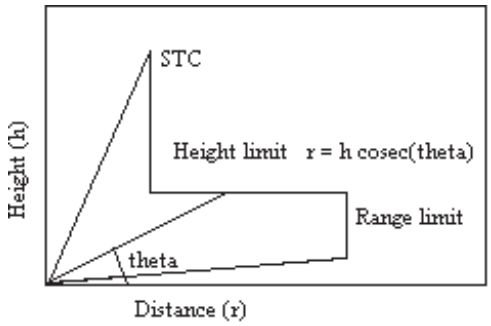

the reflector antenna in its various forms, phased arrays (passive, active and digital), endfire antennas, and lenses. They all have seen application in radar at one time or other. These antennas differ in how the radiated beam is formed and the method by which the beam is steered in angle. Steering the antenna beam can be done mechanically (by physical positioning the antenna) or electronically (by using the phase shifters with a fixed phase array). The relatively simple parabolic reflector (similar to the automobile headlight or the search light) in one form or other has been a popular microwave antenna for conventional radars. A parabolic reflector can be a paraboloid of revolution, a section of a paraboloid, a parabolic cylinder, Cassegrain configuration, parabolic torus, or a mirror scan (also called polarization-twist Cassegrain). There have also been applications of spherical reflector, but only for special limited purposes.

The mechanically rotating array antenna was the basis for the most of the lower frequency air surveillance radars that saw service early in world war II. They were eventually replaced by parabolic reflector antennas when radar frequencies increased to microwave region during and just after World War II. In the 1970s the mechanically scanned planar array antenna reappeared, but at microwave frequencies with slotted waveguide radiators or printed circuit antennas rather than dipoles. The mechanically scanned planar array is found in almost all 3D radar antennas, low sidelobe antennas, and in airborne radars where the antenna is fitted behind a radome in the nose of the aircraft. (A planar aperture allow a larger antenna to be used inside the radome than is practical with a parabolic reflector.)

Starting in the mid-1960s the electronically steered array antenna began to be employed for some of the more demanding military radar application. It is the most interesting and the most versatile of the various antennas, but it is also more costly and more complex.

2. Mechanically scanned antenna systems

To get the desired volumetric coverage of the radar, the beam of the radar antenna need to be steered in the desired direction. Mechanical scanning is a method of positioning / steering an electromagnetic beam in space by a mechanical rotation of the antenna aperture. During world war II, there were many breakthroughs in terms of realizing the radar system with an ability to detect and give the range and azimuth information of the enemy fighter aircrafts & other airborne hostile targets. Most of the radars developed during 40s to 60s were using either mechanically scanned reflector antennas (Dish antennas) or array antennas. Radar development for military applications in India was started in 80s and since then variety of mechanically scanned antenna systems were developed. Some of the significant developments are elaborated in the coming paragraphs.

2.1. *Mechanically scanned reflector antennas*

2.1.1. *Design considerations of doubly curved reflector antennas*

Rotating search radar requires a narrow pencil beam in azimuth and a wide shaped beam in elevation. In azimuth plane, the beam width is narrow and the coverage is obtained by mechanically rotating the antenna by 360°. Shaped beam in elevation is required to illuminate wide regions in the vertical plane, besides taking care of echo coming from a target flying at a constant altitude. For a target of given radar cross section (RCS) σ, taking into account the maximum range of a system, a coverage diagram of the type shown in Figure 1 is required[5]. Since the distance r is proportional to cosec (θ), the pattern obtained is called a cosecant-squared pattern (when energy is considered). From this coverage diagram the required elevation pattern can be derived as shown in Figure 2. This is determined by considering three distinct regions viz., (i) range

Figure 2: Elevation angle vs range coverage diagram.

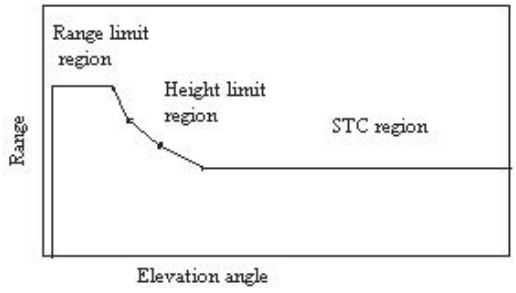

Figure 3: Geometry of ray reflections (central section).

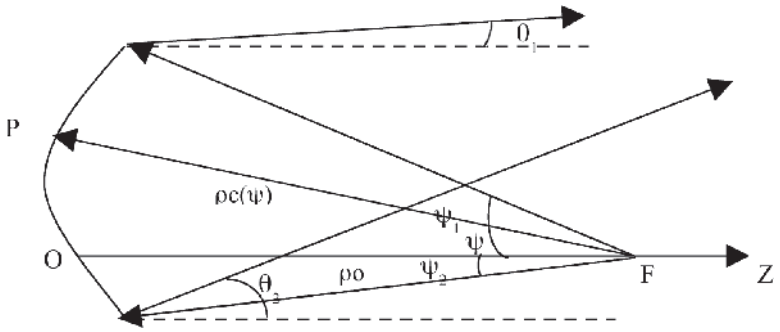

limit (ii) height limit and (iii) STC (Sensitivity Time Control). To produce such a shaped beam, doubly curved reflector antenna is convenient.

The aperture size of a doubly curved reflector antenna is usually determined by assuming a situation so that a section of reflector is shaped such that the –3 dB points of required pattern will hit the two corners of range limit portion of coverage curve[5]. But in the present study, the aperture size is determined by considering a situation wherein; the power level of lower than –3 dB points hits the top corner of the diagram shown in Figure 1 With this approach, the required aperture size of reflector becomes much smaller than the usual one. Hence, the coverage can be realized with limited aperture.

The reflector dimensions are chosen based on the azimuth and elevation beam width requirements. The physical dimensions chosen are: 3.2 m in azimuth and 1.0 m in elevation.

The central section curve decides the elevation pattern. The antenna is required to focus the energy in the azimuth plane to provide the necessary gain. The central section curve designed on the basis of geometrical optics and energy balance principles is modified by means of analysis methods. Transverse strips are designed for producing narrow beam width in azimuth plane. Azimuth plane focusing is be achieved by focal point strips.

2.1.2. *Design procedure*

The azimuth profile of reflector is designed so as to produce a focused beam. The elevation coverage is shaped to produce cosecant pattern. Considering the total reflector as symmetrical with respect to the elevation plane, determination of central section is the first step in the design process.

(a) Design of the central section. The design of the central section profile is based on the principle of geometrical optics and energy balance principles[6]. Diffraction phenomenon is not taken into consideration in the present design. The central section curve, derived on the basis of geometrical optics is modified by means of analysis methods.

The cross section configuration of the reflector, the feed position and the rays are shown in Figure 3. The z-axis is taken in the horizontal direction; F indicates the position of the feed.

Positive angles are measured in the clockwise sense. The reflector subtends a total angle of $\psi_2 - \psi_1$

Figure 4: Profile of the central section.

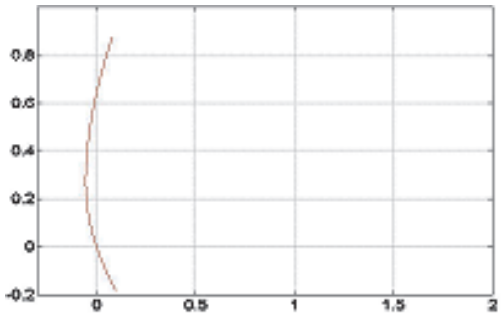

at F. ρ is the radius of curvature from F to any arbitrary point P on the curve. From the law of reflections[6,7],

$$\frac{d\rho}{\rho d\psi} = \tan\left(\frac{\psi+\theta(\psi)}{2}\right) = \tan\left(\frac{\beta}{2}\right). \quad (1)$$

The relation between $\rho_c(\psi)$ and β is computed from above equation,

$$\log_e\left(\frac{\rho_c(\psi)}{\rho_0}\right) = \int_{\psi 1}^{\psi 2} \tan\left(\frac{\beta}{2}\right) d\psi \quad (2)$$

where $\rho_0 = \rho_c(\psi_0)$; ($\psi_0 = 0$, in present case).

Solution of this equation requires knowledge of $\theta(\psi)$ vs. ψ. Considering a small wedge around the central section and the energy in the primary and secondary angular wedges, we can write[6,7]

$$G(\psi)\, d\psi = K\, P(\theta)\, d\theta\, \rho_c(\psi). \quad (3)$$

Here, $P(\theta)$ is the far field pattern between the angular limits $\theta 1$ and $\theta 2$; $G(\psi)$is the feed illumination function and K is the constant of proportionality. The following relation governs the constant of proportionality[7],

$$K = \frac{\int_{\psi 1}^{\psi 2} \frac{G(\psi)}{\rho_c(\psi)} d\psi}{\int_{\theta 1}^{\theta 2} P(\theta) d\theta}. \quad (4)$$

The final equation to be solved for determining $\theta(\psi)$ vs. ψ relation is

$$\frac{\int_{\psi 1}^{\psi} \frac{G(\psi)}{\rho_c(\psi)} d\psi}{\int_{\psi 1}^{\psi 2} \frac{G(\psi)}{\rho c(\psi)} d\psi} = \frac{\int_{\theta 1}^{\theta} P(\theta) d\theta}{\int_{\theta 1}^{\theta 2} P(\theta) d\theta}. \quad (5)$$

To determine the reflector central section profile, it is necessary to assume $\rho_{c1}(\psi)$. As an initial guess, let

$$\rho_{c1}(\psi) = \frac{2F}{(1+\cos\psi_1)}, \quad (6)$$

which is the equation of a parabola. Using this assumption integration can be performed to determine $\theta(\psi)$vs. ψ. $\rho_{cp-1}(\psi) = \rho_{cp}(\psi) \pm \varepsilon$ is achieved (till the specified limits of error, ε is reached) through an iterative process by using the initial values of $\theta(\psi)$vs. ψ.

To get maximum gain from the reflector, the feed is to be tilted such that the reflector is illuminated equally on either side by the feed. A feed illumination function, which is of the form, $\cos^2\psi$ is assumed. The actual value is $G(\psi) = \cos^2 k'(\psi - \psi_0)$. This takes into consideration, tilting of the feed by ψ_0. k' accounts for the determination of –10 dB point and ψ_0 is the angle corresponding to peak of the feed intensity. The required far field elevation pattern $P(\theta)$ indicated in Figure 2 is obtained by a combination of three functions, i.e.,

$$P(\theta) = P_1(\theta) + P_2(\theta) + P_3(\theta) \quad (7)$$

where $P_1(\theta) = e^{-k_1(\theta-\theta_0)^2}$ accounts for the pencil beam portion;

$P_2(\theta) = k_2 \cos ec^2\theta$ accounts for the cosecant region and

$P_3(\theta) = k_3$ accounts for the STC region.

The integral equation is required to be solved for three regions. $P(\theta)$ from the graph may also be considered for computation. The central section curve is as shown in Figure 4.

(b) Design of transverse strips. The central section curve decides the elevation pattern. The antenna is required to focus the energy in the azimuth plane to provide the necessary gain. Azimuth plane focusing can be achieved in three

Figure 5: Radars with curved reflector antennas.

(a) Indra – PC Radar for Air Force

(b) Indra Radar for Army

ways. They are (a) Elevation angle strips, (b) Horizontal strips and (c) Focal point strips[8]. Due to size restriction of the antenna in terms of wavelength in the elevation plane, it was found during computation that the Elevation angle strips and Horizontal strips are not practical. Hence the only practical option of Focal point strips was considered. The equation for computation of focal point strips is

$$\frac{x^2}{\rho^2[\sin(\psi+\theta)/(1+\cos(\psi+\theta))]^2} + \frac{[z-\rho/(1-\cos(\psi+\theta))]^2}{\rho^2[1/(1-\cos(\psi+\theta))]^2} = 1. \quad (8)$$

Additional details of the design are given in[9]. In the following subsections we will see how these are implemented in some of radars used by the Services.

2.1.3. *Indian pulse doppler radar (INDRA)*

Indian **D**oppler **Ra**dar Pulse Compression (INDRA-PC) radar was developed in 1980s to meet Air Defence requirement of Indian armed forces. This is a mechanically scanned doubly curved reflector antenna based system for detecting low flying targets, This L Band Radar provides range and azimuth information of the target accurately. To meet the requirement of detecting targets flying at a very low altitude to a high altitude without scanning the antenna beam in elevation, an antenna has to be designed that can produce a very narrow pencil beam in azimuth and shaped beam in elevation. To synthesize such types of beam, the distribution of radiated power need to follow cosine distribution in azimuth and cosecant-squared distribution in elevation. Such type of distribution in azimuth and elevation planes were achieved by shaping the conventional reflector in both the dimensions to a doubly curved reflector antenna surfaces with a point source feed. The design of doubly curved reflector involves the realization of central section curve which is shaped to get cosec-squared pattern in elevation and a system of parabolic for focusing the beam in the azimuth plane.

In practice, such antennas are realized using metal strips instead of a solid reflector surface for reducing the wind load, ease of fabrication and weight. These metal strips can be realised as Elevation angle strips, Horizontal strips and

Figure 6: Radiation patterns of reflector antennas.

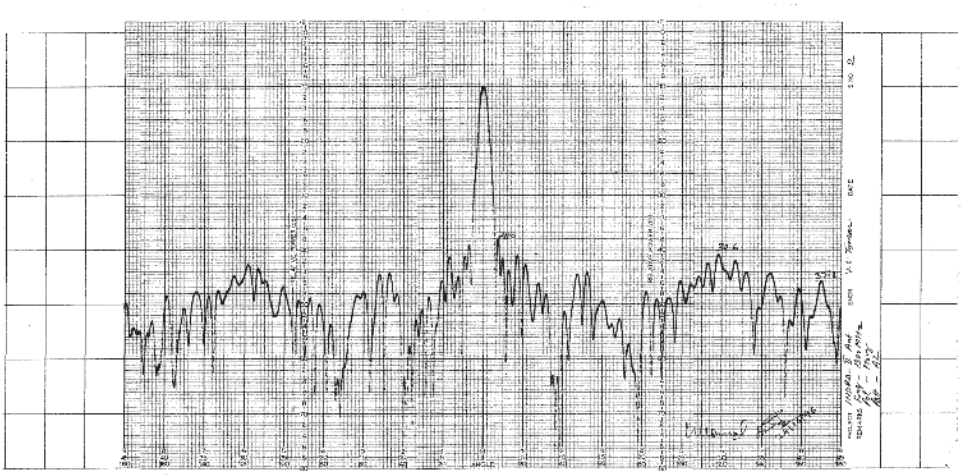

(a) Azimuth Low Side lobe beams

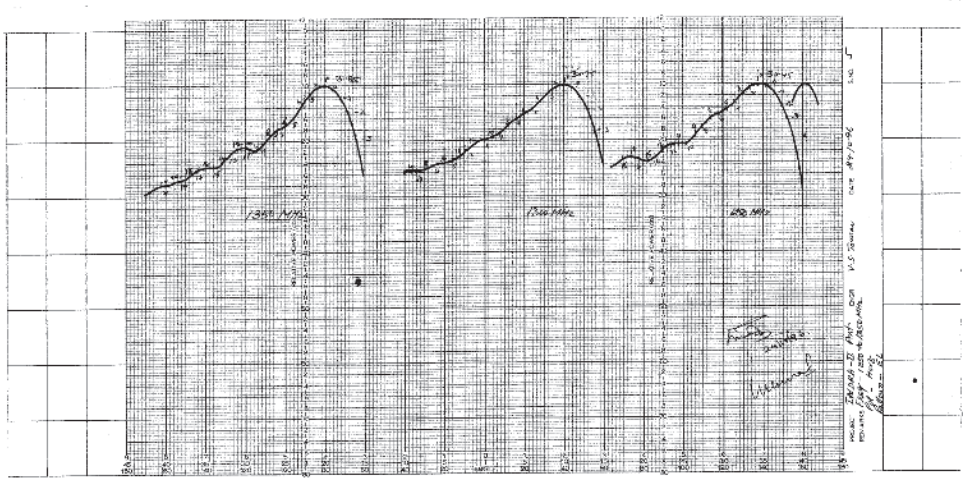

(b) Elevation Shaped Beams

focal point strips. Out of these three possible configurations, focal point strips offers the best aperture efficiency. Hence, for Indra-Radar which utilizes the doubly curved reflectors, the central section curve is synthesised to get the cosec-squared pattern in elevation as per the specifications to meet the respective coverage diagrams and focal point strips are used to realise the antenna. The radar has integrated IFF antenna in doubly curved parabolic main antenna. It has high gain feed antenna with fairly low sidelobe levels using efficient corrugated horn which supports dual polarisation. Indra Radar (Air Force & Army) alongwith their azimuth and elevation pattern is shown in Figures 5 and 6.

2.1.4. *Low level light weight radar (Bharani) for air defence*

BHARANI is a mechanically scanned doubly curved reflector antenna for low level light weight mountainous terrains. The antenna has been designed to meet the radar beam width requirement of about 5.0° in azimuth plane and a shaped beam in the elevation plane to provide elevation coverage in order to meet the detection requirements of targets flying close to ground level and up to 6000 m in altitude.

Weight and wind resistance of reflector antenna is reduced considerably by replacing the continuous surface by a grating structure. The gratings are

Figure 7: Bharani Radar Antenna system.

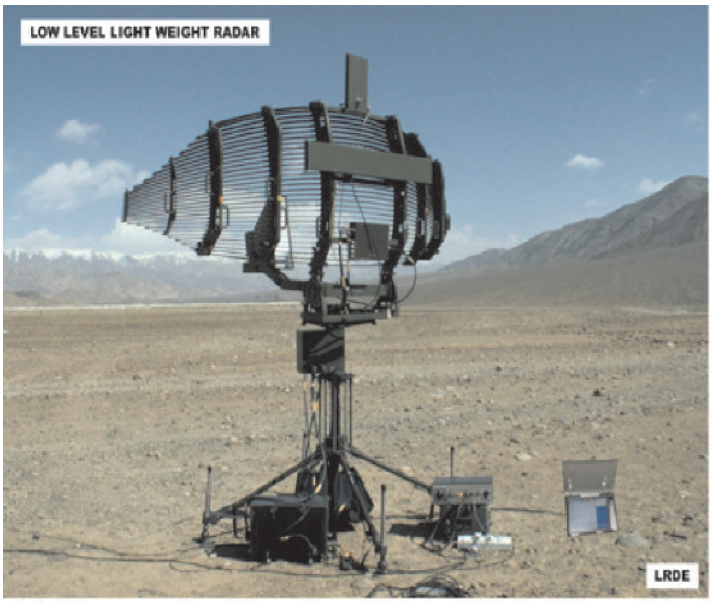

(a) Photograph of Low Level Light Weight Bharani Radar

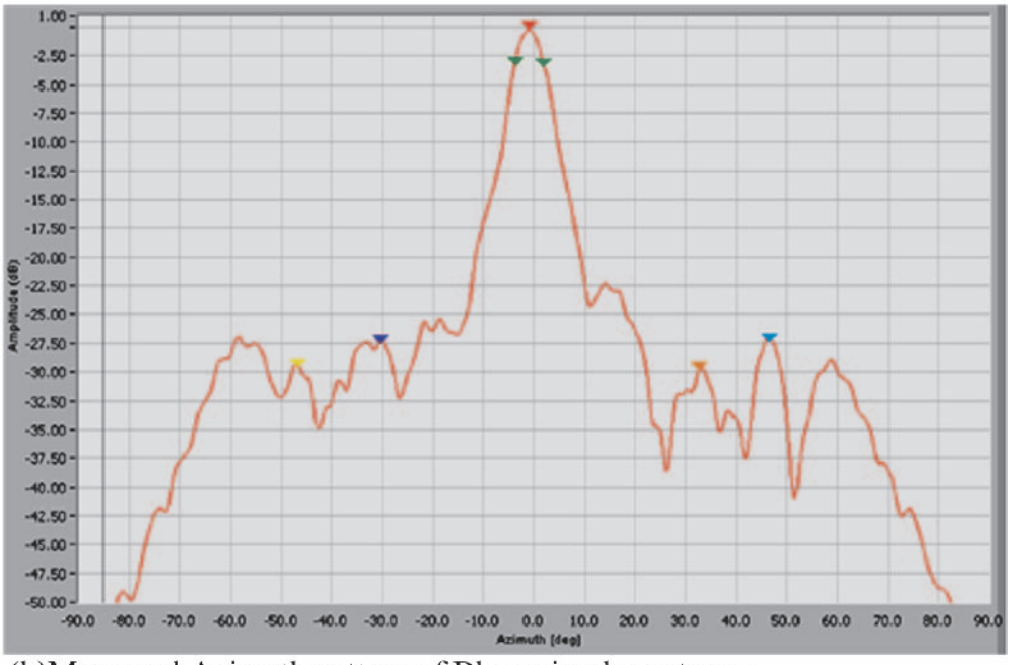

(b)Measured Azimuth pattern of Bharani radar antenna

sensitive to polarization. Edge wise strips are considered for the manufacture of main reflector antenna and is segmented into eight segments. It can be dismantled into packages to facilitate quick installation and re-location in mountainous terrain. The antenna is designed, fabricated and tested in a near field measurement set-up. Photograph of the Antenna alongwith measured azimuth and elevation patterns are shown in Figure 7.

2.2. *Mechanically scanned slotted waveguide array antenna*

Over last two decades LRDE have been concentrating on the development of various airborne radars for DRDO's front-line projects like airborne surveillance platform (ASP), light

Figure 7: *continued..*

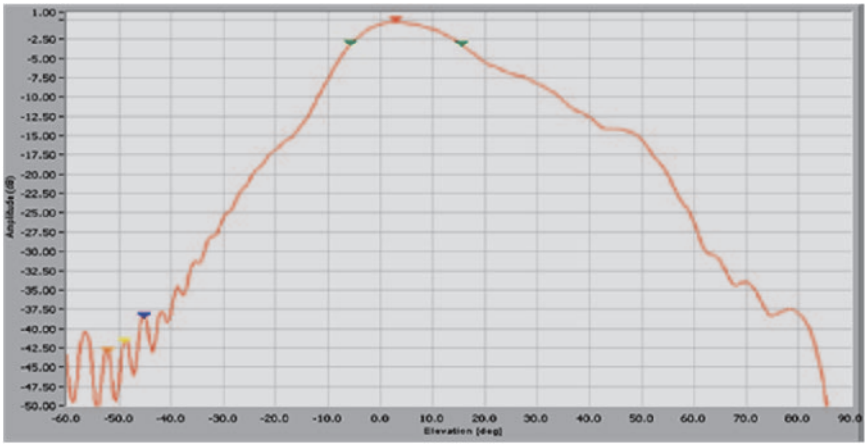

(c) Measured elevation pattern

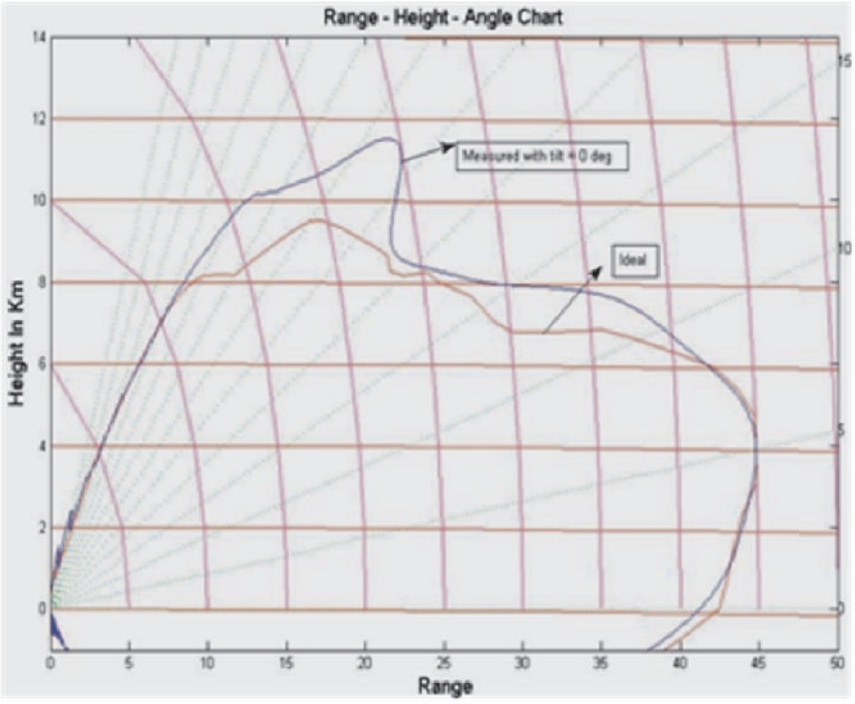

(d) Comparison of measured, dersired and broad-beam elevation patterns

combat aircraft (LCA), advanced light helicopter (ALH), synthetic aperture radar for unmanned aerial vehicles (UAVs) and for various missile seeker heads. There was a strong demand for high gain and efficient antennas for these radar applications. Since waveguides provide exceptionally low path loss and accurately repeatable array elements, waveguide slotted arrays have been attractive candidates for high power, high efficiency, rugged and compact array antennas.[4,10–12]

Performance of a very low sidelobe slotted array depends on the accuracy with which individual radiating and coupling slots are characterized. Due to the complex nature of the boundary value problem encountered in the analysis of radiating and coupling slots, accurate theoretical and numerical analysis were required to achieve high degree of accuracy. The open literature available on the subject was very limited and certainly not sufficient for realizing an antenna. Only limited radar houses all over the world have this technology but refused to share their knowledge and expertise for designing

and developing such antennas. Hence LRDE resort to developing the technology. The goal was to create waveguide slotted array antenna technology from the fundamentals by developing the necessary electromagnetic analysis and solve the complex boundary value problem numerically using Method of Moment (MoM) / Finite Element method (FEM) thereby creating a strong and versatile CAD based design tool which with ease can be used to produce an optimised antenna of the desired characteristics for various applications.

To meet the stringent electrical and mechanical requirements, a design methodology has been developed at LRDE. Based on extensive electromagnetic modelling using Method of Moments and Finite Element Techniques which offers high degree of accuracy, a computer aided design tool followed by computer controlled slot machining and fabrication methodologies have been developed. Various joining processes like dip brazing, vacuum brazing, adhesive bonding etc, to join up to four layers of antenna have been developed which are very critical processes.

2.2.1. *Array architecture and design issues*

The multi layer resonant slotted waveguide planar array consists of parallel rectangular waveguides into which longitudinal—offset slots have been cut as a basic radiating element. The radiating slots in each waveguide are spaced one half guide wavelength apart and are sequentially offset on opposite side of the waveguide centre line in order to have equiphase excitations. It requires coupling slots as feeding elements in addition to radiating slots. A centered-inclined slot located in the common broad wall of radiating and feeding waveguide is widely used coupling element because of its better behaviour off-resonance. The planar array consisting of N radiating waveguides having M radiating slots, stacked side by side to make a planar array of the radiating aperture $M \times N$. The non-standard radiating and feeding waveguide dimensions are chosen in such a way that inter element spacing in both the waveguides (i.e. radiating waveguide and feeding waveguide) remains same. Depending upon the requirements, the entire aperture of the planar array can be divided into number of subarrays to get the required bandwidth. The radiating waveguides of each subarray are short circuited at both ends and an additional waveguide called feed guide passes perpendicular to and underneath radiating waveguides is used to feed radiating slots via coupling slots (called feed layer coupling slots). The coupling slots, one for each radiating waveguide are situated in the common broad wall of the two waveguides. These slots are spaced half a guide wavelength apart in the feeding waveguide and are sequentially inclined with opposite tilts to achieve equi-phase excitation of coupling slots and therefore of radiating waveguides. These feed lines are connected to the unequal power divider network through another layer of coupling slots.

The design of a high performance slotted waveguide array antenna requires proper aperture distribution in amplitude and phase and carefully controlling and compensating for the many error sources in the design, fabrication, assembly and joining. As both the input VSWR and aperture distribution depend on the active admittances/impedances of all slots in the array, utmost care has to be taken for isolated radiating and coupling slot characterisations. This individual slot characterisation is then fed in the planar array design module. The entire design and development philosophy along with the design principles can be summarised as follows:

2.2.2. *Method of moments analysis for rectangular waveguide slots*

As described in the previous section, there are mainly two types of waveguide slots widely used in designing slotted waveguide array antennas, longitudinal offset radiating slots (radiating to free space) and centered-inclined coupling slot located in the common broadwall of two rectangular waveguides placed orthogonal (or non-orthogonal) to each other. The predicted performance of a slotted waveguide array antenna heavily depends on the accuracy at which individual radiating and coupling slots are analysed/characterised. As method of moments offer great advantages in this context, a comprehensive MoM analysis is carried out to characterise these slots. A brief of the same is discussed underneath.

The slot is assumed to be excited by TE_{10} mode from a matched generator and terminated in a matched load. The co ordinate system of a centered-inclined slot coupler is shown in the Figure 8. The structure is divided into regions A, B and C where A is the mainline waveguide region, B is the slot (or cavity) region and C is branch line region. In region A and C, slot is completely shorted and magnetic current sheets $M_{\alpha 1}$ and $M_{\alpha 2}$ are placed in its location at $y = b^-$ and $y = b + t^+$. In region B both slot apertures are shorted by magnetic current sheets $-M_{\alpha 1}$ and $-M_{\alpha 2}$. The problem is solved by making use of couple of integral equations for slot electric field which can be arrived at by equating magnetic fields on the two sides of the slot interface. The slot electric field is assumed to be varying along the length with no variation across the width.

Figure 8: (a) Waveguide & Cavity Regions; (b) Coordinate system of the slot.

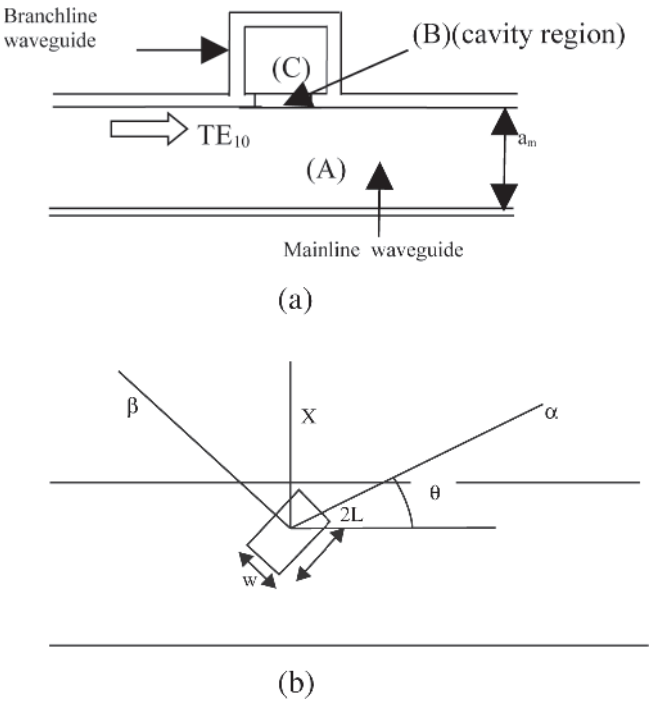

A pair of coupled integral equations obtained after enforcing the continuity of longitudinal magnetic fields across each slot aperture is

$$H_{\alpha}^{inc} + H_{\alpha 1}^{scat} = H_{\alpha 1}^{c} \tag{9}$$

$$H_{\alpha 1}^{scat} - H_{\alpha 2}^{c} = 0. \tag{10}$$

These magnetic field components are described next. H_{α}^{inc} is the TE_{10} incident tangential magnetic field, given by

$$H_{\alpha}^{inc} = A_{10} e^{j\beta_{10} Z} \left[j\cos(\pi x/a_m)\cos\theta - \frac{\beta^{10}}{\pi/a_m}\sin(\pi x/a_m)\sin\theta \right] \tag{11}$$

where a_m is the mainline waveguide's "a" dimension.

In eq. (9) and (10) $H_{\alpha 1}^{scat}$ is the scattered magnetic field inside the waveguide and is expressed in terms of aperture magnetic current $M_{\alpha 1}$ through respective Green's function.

$$H_{\alpha 1}^{\text{scat}} = \int_{s'}\int [\cos\theta \sin\theta][G^{\text{main}}] \times [\cos\theta \sin\theta.]^{T} M_{\alpha 1} ds'. \tag{12}$$

The integration is performed over the interior slot aperture s_1.

In eq. (12), $[G^{\text{main}}]$ is the internal mainline waveguide Green's function which is similar to that of [13]. $H_{\alpha 1}^{c}$ and $H_{\alpha 2}^{c}$ are the lower and the upper aperture fields in the cavity due to the magnetic currents $-M_{\alpha 1}$ and $-M_{\alpha 2}$ respectively and are given by

$$H_{\alpha 1}^{c} = -\int_{s1}\int G_{s\alpha\alpha}^{c} M_{\alpha 1} ds' - \int_{s2}\int G_{e\alpha\alpha}^{c} M_{\alpha 2} ds' \tag{13}$$

$$H_{\alpha 2}^{c} = -\int_{s1}\int G_{e\alpha\alpha}^{c} M_{\alpha 1} ds' - \int_{s2}\int G_{s\alpha\alpha}^{c} M_{\alpha 2} ds' \tag{14}$$

where $G_{e\alpha\alpha}^{c}$ and $G_{s\alpha\alpha}^{c}$ are cavity region Green's function[14].

Similarly, $H_{\alpha 2}^{\text{scat}}$ is the tangential magnetic field in the region C and is computed from magnetic current $M_{\alpha 2}$ using branch line internal waveguide Green's function G^{branch} i.e.,

$$H_{\alpha 2}^{scat} = \int\int [\sin\theta\cos\theta][G^{branch}] \times [\sin\theta\cos\theta]^{T} M_{\alpha 2} ds' \tag{15}$$

where $[G^{\text{branch}}]$ is expressed in terms of branch line waveguide dimensions.

Figure 9: 3D Impedance curves of slot elements (Slot impedance plotted against slot inclination and slot resonant length (a-Resistance, b Reactance).

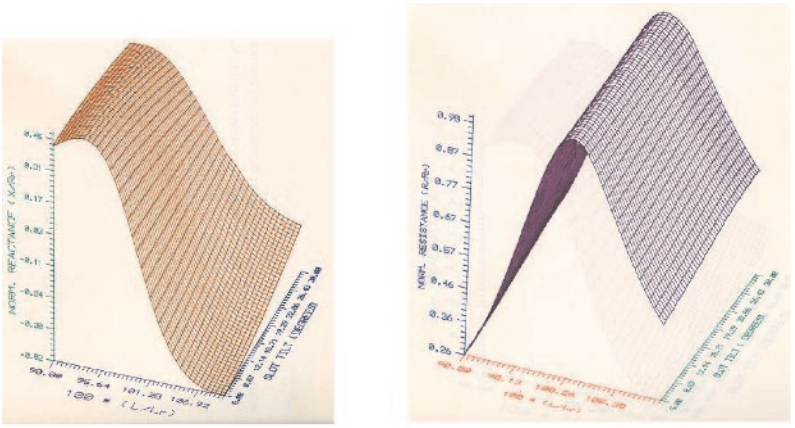

(a) (b)

The integral equations (9) and (10) are solved by method of moments using Garlerkin's method[15]. It has been found that around the first resonance the field within the slot is essentially sinusoidal and hence trigonometric functions can be chosen as basis functions. Let

$$M_{\alpha 1} = \sum_{q=1}^{N} A_q \sin\left[\frac{q\pi(\alpha_1 + L)}{2L}\right] \qquad (16)$$

$$M_{\alpha 2} = \sum_{q=1}^{N} B_q \sin\left[\frac{q\pi(\alpha_1 + L)}{2L}\right] \qquad (17)$$

where A_q and B_q are unknown coefficients.

As Galerkin method is used, the weighing function should be of the same type as basis functions, namely

$$w_p = \sin\left[\frac{p\pi(\alpha_1 + L)}{2L}\right]. \qquad (18)$$

The basis function needed to satisfy the same boundary conditions as satisfied by the magnetic current sources in order to converge magnetic current expansion series. The moment method converts the integral equations in to matrix which is then solved for unknown coefficients A_q and B_q. The field distribution on the surface of the slot can be obtained once unknown coefficients are solved.

Number of software packages (few of them mentioned below) for slot characterisation, using above described Method of Moment technique has been developed. All these softwares are menu driven, user friendly, valid for wide frequency band and takes care of any standard/non-standard waveguide dimensions.

The impedance properties of offset radiating slots are characterised as a function of frequency, waveguide dimensions, slot widths, slot offset and slot length. A theoretical analysis of the broad wall radiating slots for various off sets from the centre line of a rectangular waveguide is carried out. Pertinent integral equations taking into account finite wall thickness have been developed and solved for the slot aperture E-field using the Method of Moments. A suitable software package called CoBRa (**C**haracterization **o**f **B**roadwall **Ra**diating Slots) has been developed based on MOM analysis[16] .

In addition, the impedance properties of radiating slots covered with a dielectric radome are characterised as a function of slot offset and length[17]. A software package called COBRA-DC[18] has been developed based on MoM analysis. Furthermore, the impedance properties of centered inclined coupling slots located in the common broadwall of two rectangular waveguides placed orthogonal to each other are characterised as a function of slot tilt and length[19]. A rigorous analysis of finite wall thickness dissimilar orthogonal rectangular waveguide coupled through a centered inclined slot has been made[19–21]. The procedure begins with the development of fundamental integral equations using Schelkunoff's equivalence principle, dyadic Green's function formulations in the different waveguide regions and appropriate boundary conditions. The coupled integral equations are solved using Method of Moments with entire basis and testing function. With a great amount of analytical and computational effort, an efficient

and accurate software package called CoBICS (**C**haracterization **o**f **B**roadwall **I**nclined **C**oupling **S**lots) has been developed[22]. The existing theory has been modified to make it computationally efficient[19–22]. This package computes various coupling slot characteristics, which include slot resonant length, slot impedance, back scattered and forward scattered coefficients and coupling over a range of waveguide dimensions, slot dimensions, slot inclinations and frequency. An extensive validation of the software has been made theoretically by comparing it with published results in the literature. A 3-D impedance curve as a function of slot tilt and slot length generated using this software is shown in Figure 9.

2.2.3. *Planar array design*

2.2.3.1. Aperture Distribution. The choice of a suitable aperture distribution for the design of the antenna is arrived at after studying the various specification of the antenna. The main parameters of the antenna which are influenced by the aperture distribution are :

Side lobe level in Azimuth and Elevation Planes
−3 dB Beamwidths in Azimuth and Elevation Planes
Gain

Depending on the geometry of the antenna an appropriate aperture distribution is chosen. Of the various types of distributions available, Taylor's distribution is practically optimum to implement and realise during the actual fabrication[23]. A suitable Taylor's aperture distribution has to be determined to achieve the desired design specifications. Care need to be taken to have enough margin in the chosen distribution for all the parameters to allow for errors during the practical realization of the antenna.

2.2.3.2. Design of radiating aperture. The basic planar design yields both slot offset with respect to the axis of the waveguide and length of the slot that will give the required aperture distribution and impact match. The design should also take care of both internal and external mutual couplings. The internal mutual coupling is taken care at the time of slot characteristics by adding the higher order modes. The external mutual coupling, of course, has to be considered using dipole model or slot model using method of moments. The most time consuming part in the design is the computation of external mutual coupling apart from radiating and coupling slot characterizations. There are various algorithms which can be used to reduce the computation time for external mutual coupling[24].

The design procedure for planar array is based on the system of equations developed by Elliott[10]. The basic design equations for an $M \times N$ element planar array are given by

$$Y^a_{mn}/G_o = k_1 f_{mn} \sin(kl_{mn})\, V^g_{mn}/V_{mn} \quad (19)$$

$$Y^a_{mn}/G_o = k_2 f^2_{mn}/Z^a_{mn} \quad (20)$$

where

$$k_1 = j[8(a/b)/(\pi^2 \eta G_o \beta/k)]^{1/2} \quad (21)$$

$$k_2 = 292(a/b)/(0.61\pi\beta/k) \quad (22)$$

and

$$f_{mn} = (\cos\beta l_{mn} - \cos kl_{mn}) \frac{\sin \pi x_{mn}/a}{\sin kl_{mn}}.$$

The other notations are defined in[10]. The active impedance of the nth equivalent loaded dipole is given by

$$Z^a_{mn} = Z_{mn} + Z^b_{mn} \quad (23)$$

in which

$$Z^b_{mn} = \sum_{m'=1}^{M} \sum_{n'=1}^{N} \frac{V^2_{m'n'} \sin(kl_{m'n'}) Z^{m'n'}_{mn}}{V^2_{m'n'} \sin kl_{mn}} \quad (24)$$

is the mutual coupling and

$$Z^{mn}_{mn} = Z_{mn} + Z^1_{mn} \quad (25)$$

is the loaded self impedance of the dipole. Z^1_{mn} the load impedance in series at the terminals of the nth dipole. It is necessary to determine Z^{mn}_{mn} as a function of the length and offset of the complementary wave guide-fed slot.

It is assumed that the input admittance to the mnth slot is the same whether all other slots are

- present and short circuited
- present and open circuited or totally absent

Experiments show that this is a good assumption. It can be inferred from that

$$Z^{mn}_{mn} = K_2 f^2_{mn} / Y_{mn} / G_0 \quad (26)$$

in which $Y_{mn} / G_0(x_{mn}, l_{mn})$ is the isolated self admittance of the m, nth slot. Thus if one measures the Y_{mn} / G_0 for an isolated slot as a function of its length and offset, eq. (25) can be used to deduce the function $Z_{mn}\ (x_{mn}, l_{mn})$ needed for use in eq. 19.

If one lets $y = l/l_r$ represent the abscissa scale, then

$$h(y) = h_1(y) + jh_2(y) \tag{27}$$

can symbolize the complete sum of these universal curves. With $g(x)$ taken to mean the normalized resonant conductance as a function of offset, it follows that

$$Y/G_0 = g(x)\ h(y). \tag{28}$$

To interpret variable y, it is necessary to know the relation between the resonant length and offset. This is characterised by the function

$$v(x) = kl_r(x). \tag{29}$$

Now, the equation (25) can be written in the form

$$Z_{mn}(X_{mn},\ y_{mn}) = K_2\ f_{mn}^2(x_{mn},\ y_{mn}) \Big/ g(X_{mn})\ h(y_{mn}) \tag{30}$$

in which,

$$f_{mn}(x_{mn}, y_{mn}) = \left[\frac{\cos[(\beta/k)y_{mn}\, v(x_{mn})] - \cos[y_{mn}\, v(x_{mn})]}{\sin[y_{mn}\, v(x_{mn})]}\right] \times \sin(\pi x_{mn}/a). \tag{31}$$

Depending on the pattern requirements (ie., distribution in azimuth and elevation plane to get the required side lobe level), the radiating slot excitation were obtained using Taylor distribution. The above design equations were used to determine length and displacement of each slot in order to achieve the required excitations and proper input match taking into account the mutual coupling effect among the radiating slots in a radiating waveguide.

2.2.3.3. Design of first layer and second layer of coupling slots. The design of input coupling slots is separated from the synthesis of radiating slots in the radiating waveguides by assuming the required excitations in all radiating waveguides and also by choosing a certain value of the normalized input matches for all the radiating waveguides. A previous study has shown that a choice of Yin = 1 yields an optimum bandwidth for pattern performance. A novel technique has been developed to design coupling slots such that all the radiating waveguide excitations are maintained with reference to the centre of the coupling junctions with the required input match at the feeding port.

It is desirable to know the coupling behaviour of centered-inclined slot coupler to be used in designing the first layer of the antenna. The centered-inclined slot located in the common broadwall of crossed rectangular waveguiedes can be represented as a four port coupler. The scattering matrix of the four port coupler may be expressed in terms of only three unknowns: S_{11}, S_{13} and S_{33}. At resonance all S-parameters may be expressed in terms of S_{11}. A four port coupler can be represented as:

$$\begin{bmatrix} b_1 \\ b_2 \\ b_3 \\ b_4 \end{bmatrix} = \begin{bmatrix} S_{11} & 1-S_{11} & S_{13} & -S_{13} \\ 1-S_{11} & S_{11} & -S_{13} & S_{13} \\ S_{13} & -S_{13} & S_{33} & 1-S_{33} \\ -S_{13} & S_{13} & 1-S_{33} & S_{33} \end{bmatrix} \times \begin{bmatrix} a_1 \\ a_2 \\ \Gamma_3 b_3 \\ \Gamma_4 b_4 \end{bmatrix}. \tag{32}$$

This scattering matrix is used in the set of equations $[b] = [S][a]$ in which $[a]$ is the set of voltage waves incident on the four ports, with $[b]$ the corresponding set of backscattered waves. S_{11} is obtained through method of moments analysis. We are interested in applying (32) to the case of planar array of resonantly spaced longitudinal slots. In that case each slot in the array can be represented by a normalized active admittance, a quantity which includes mutual coupling as well as self admittance. For that part of a branchline being fed by port #3, the sum of these active admittances can be represented by Y_3 (normalized wrt G_0) in a reference plane $\lambda_g/4$ away from the center of the coupling slot. Similarly, for that part of the same branchline being fed by port #4, the sum of active admittances can be represented by Y_4, also referenced in a plane $\lambda_g/4$ from the center of the coupling slot, but on the other side. All port references are at the center of the slot. We can express the relation between b and a waves solving the above matrix as follows:

$$\begin{aligned} b_1 &= S_{11}a_1 + (1-S_{11})a_2 + S_{13}a_3 - S_{13}a_4 \\ b_2 &= (1-S_{11})a_1 + S_{11}a_2 - S_{13}a_3 + S_{13}a_4 \\ b_3 &= S_{13}a_1 - S_{13}a_2 + S_{33}a_3 + (1-S_{33})a_4 \\ b_4 &= -S_{13}a_1 + S_{13}a_2 + (1-S_{33})a_3 + S_{33}a_4. \end{aligned} \tag{33}$$

If $b_1 = \Gamma_{in}\ a_1$, $a_2 = \Gamma_2$, $a_3 = \Gamma_3$ and $a_4 = \Gamma_4$, then rearranging and solving above equations, it has been found that

$$\frac{b_3}{a_1} = \frac{C_1X_4 - C_2X_2}{X_1X_4 - X_2X_3} \tag{34}$$

$$\Gamma_{in} = \frac{C_2X_1 - C_1X_3}{X_1X_4 - X_2X_3} \tag{35}$$

where

$$X_1 = 1 - S_{33}\Gamma_3 + \frac{(1-S_{33})(1-\Gamma_3)\Gamma_4}{(1-\Gamma_4)} \quad (36)$$

$$X_2 = -\frac{S_{13}\Gamma_2}{1-\Gamma_2} \quad (37)$$

$$X_3 = -\left\{ S_{13}\Gamma_3 + S_{13}\Gamma_4 \frac{(1-\Gamma_3)}{1-\Gamma_4} \right\} \quad (38)$$

$$X_4 = 1 + \frac{(1-S_{11})\Gamma_2}{1-\Gamma_2} \quad (39)$$

$$C_1 = S_{13} - \frac{S_{13}\Gamma_2}{1-\Gamma_2} \quad (40)$$

$$C_2 = S_{11} + \frac{(1-S_{11})\Gamma_2}{1-\Gamma_2}. \quad (41)$$

The series impedance representation of the slot is given by

$$Z_s = Z_{in} - \frac{1+\Gamma_2}{1-\Gamma_2}. \quad (42)$$

For a general case of coupling slot with ports 3 and 4 having admittances Y_3 and Y_4 at $\lambda_g/4$ away from the coupling slot centre, it can, using above expressions, be found that

$$Z_s = \frac{|S_{11}|_{res}}{|1-S_{11}|_{res}} (Y_3 + Y_4) \quad (43)$$

for resonant length coupling slot with any value of Γ_2, Γ_3 and Γ_4 and for non resonant length coupling slot with $\Gamma_2 = \Gamma_3 = \Gamma_4 = 0$.

An approximate model for coupling slot can be represented by transformer model. Now applying complex power flow balance condition

$$\frac{1}{2} I_1 I_1^* Z_s = \frac{1}{2} V_s V_s^* (Y_3 + Y_4) \quad (44)$$

where I_1 is the mode current in the mainline referenced in a plane coincident with the center of coupling junction; V_s is the mode voltage in the branch waveguide at a cross section $\lambda_g/4$ away from the junction center; Z_s is the mainline series impedance at the center of the slot.

Hence

$$V_s^2 = \chi^2 I_1^2 \quad (45)$$

where $\chi^2 = S_{11}/(1-S_{11})$.

For a planar array which is standing wave fed, I_1 has the same magnitude and alternating sign at successive junctions, this effect being counteracted by alternating directions of tilt of the coupling slots.

If N number of coupling slots are used to feed N radiating waveguides, then

$$\frac{V_{s1}}{\chi_1} = \frac{V_{s2}}{\chi_2} = \frac{V_{s3}}{\chi_3} = \cdots\cdots\cdots = \frac{V_{sn}}{\chi_n} = \cdots\cdots = \frac{V_{sN}}{\chi_N}. \quad (46)$$

Equation (43), (45) and (46) are key relations to be satisfied while designing the coupling slots.

The coupling waveguides are connected together through a waveguide unequal power divider network, which takes care of distribution and matching. The unequal power divider network is based on H-plane tee junction with two irises, first to split the incoming power to two output ports and the second to match the input port. A number of such H-plane tee junctions in conjunction with different types of bends are used to design single/double layered 1:n unequal power divider network within the space available. The entire design can be carried out using FEM based commercial software package HFSS[25]. **U**sing this, a planar magic tee junctions has also been developed and implemented[26].

2.2.4. *Fabrication, assembly and joining*

Computer controlled precision machining has been established to achieve the stringent mechanical tolerances required for this class of antenna. The complicated three dimensional multi layer structure of the slotted arrays have been of great concern mechanically as it requires perfect electrical contact at joining and high accuracy of alignment required in assembling the various parts distributed in different layers of the antenna. A novel assembly and joining technology for of this class of multi layer array antenna has been developed using dip-brazing and conductive adhesive bonding techniques. The conductive adhesive bonding technique has resulted in zero defect product as compared to conventional dip brazing or vacuum brazing processes which also requires huge initial investment and maintenance cost.

2.2.5. *Measured results of antennas systems delivered*

The complete evaluation of the antenna is done in LRDE's Microwave measurement facilities (using HP VNA/PNA), in-house developed indoor near field test facilities (PNFM, APNFM & SNFM) and outdoor antenna test range. Using these measurement facilities antenna input VSWR, antenna gain, two and three dimensional co-polar radiation patterns in all the plane of cuts, cross polar patterns, contour plots etc can be obtained. Apart from the normal measurements, software

Figure 10: Circular two plane monopulse array antenna in X- band for LCA.

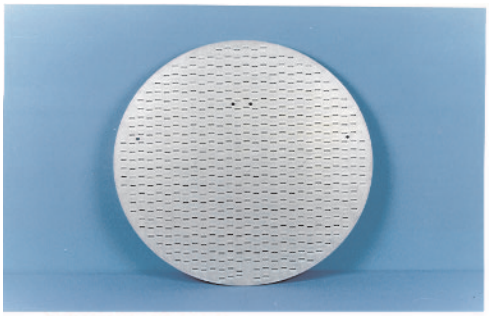

(a) Front view

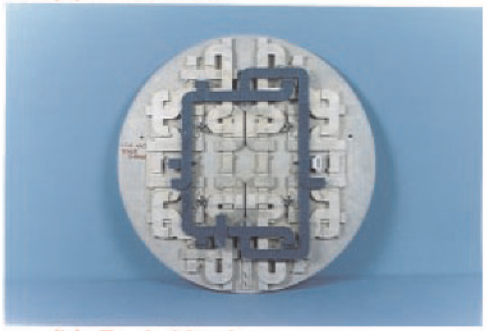

(b) Backside view

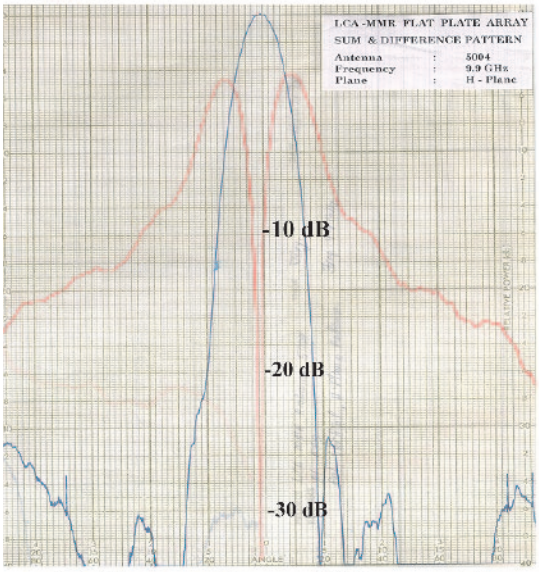

(c) Measured Sum & Difference Pattern of LCA-MMR antenna

tools have been developed to predict the aperture field (amplitude and phase) distribution utilising the planar near field measured data through inverse transformation. This technique helps in diagnosing the fault distribution.

Based on the above design methodologies and number of softwares developed, slotted arrays for ASP in S-band (Size: 6200 mm × 1200 mm, Sidelobe level < -35 dB (peak), < -45 dB (avg.) and gain > 34 dB), LCA-MMR in X-band (size: 650 mm dia, side lobe level < -30 dB (peak), < -45 dB (RMS), gain > 34 dB), X-Band array for missile applications (size: 180 mm dia, SLL < -32 dB (peak), gain > 22.5 dB), Ku-band for missile seeker head applications (size: 240 mm dia, SLL < -26 dB (peak), Gain > 28 dB), Maritime patrol radar for ALH in X-band, Battle Field Surveillance Radar and Fly Catcher Radar for M/s Bharat Electronics

have been developed and tested successfully. All the antennas developed meet all the technical requirements and are comparable to the existing antennas all over the world. A slotted waveguide array antenna for maritime patrol radar is being developed for Poland under DRDO export program. The representative test results of these antennas are shown in Figures 10 to 13. The technology has made the country self reliance (100% indigenous) in the field of slotted waveguide arrays. The product out of this technology is being used extensively for various Ground / Airborne / Missile Radars developed by DRDO.

Significant Features of the Flat Plate Antenna System for Multi Mode radar of LCA (Figure 10) include:

X-band, 600 MHz band width
Vertically polarized
Subarraying and multi layer feed network for enhancing the bandwidth
Two plane monopulse capability
Integrated IFF & Guard
Fabrication through the use of precision machining & dip-brazing
SLL : < -30 dB (peak), < -45 dB (rms)
Gain > 34 dB
Power handling : 10 KW (peak)
Size : 650 mm dia, weight : 4.8 Kg

Major Features of the Horizontally polarized slotted waveguide Antenna for Maritime Patrol Radars (Figure 11) include:

X-band, 500 MHz band width
Horizontally polarized
Subarraying and multi layer feed network for enhancing the bandwidth
Az plane monopulse capability
Fabrication through the use of precision machining & adhesive bonding
SLL : < -28 dB (peak), < -40 dB (rms)
Gain > 30 dB
Power handling : 10 KW (peak)

Significant Features of the Monopulse Array Antenna for Missile Seeker Head (Figure 12) include

Ku-band, 500 MHz band width
Non-standard reduced height waveguides for compactness & light weight
Monopulse comparator using planar magic tees
Fabrication through the use of precision machining & adhesive bonding
SLL : < -26 dB (peak), < -40 dB (rms)
Gain > 28 dB
Power handling : 10 KW (peak)
Size : 220 mm dia, weight < 500 gms

Some features of the Non-Resonant slotted waveguide Array Antenna for Airborne Surveillance Radar (Figure 13) include

S-band, 400 MHz
Vertically Polarized
Ultra Low side lobes (< -40 dB peak, -50 dB (rms)
Size : 6 m $\times$ 2 m

2.3. *Microwave multi beam antenna for 3D surveillance radars Rohini and Revathi*

Multi beam antennas (MBA) is the most critical sub system of 3-D radars where it has become possible to generate three co-ordinates of the object i.e., distance, azimuth and height. A multi beam antenna is one with a capability to form many beams in different directions from a single aperture. Mechanically Scanned Multi Beam Antenna System for long range 3D Surveillance Radars Rohini (Indian Army) and Revathi (Indian Navy) were also developed. The design and development of a antenna system capable of forming a very low side lobe narrow beam in azimuth (Peak SLL < -35 dB, Average SLL < -50 dB), shaped beam in elevation during transmit mode of operation for the required elevation coverage and multiple low side lobe beams of varying beam widths (SLL < -30 dB) simultaneously in elevation during receive from a single aperture is described here. A comprehensive method for designing a 4 meter by 2 meter planar array of air-dielectric stripline fed triplate dipole arrays to produce a very low side lobe pencil beam in azimuth, a shaped beam forming network to produce a near cosecant squared pattern in elevation during transmit mode of operation and a Blass beam forming network to produce 'N' no. of beams (Typically 6 to 8 beams) simultaneously in elevation during receive mode of operation has been described. A schematic of multi beam antenna system is shown in Figure 14.

The antenna system consists of mainly three core elements i.e. a planar array, a shaped beam-forming network (to produce cosecant squared pattern in elevation during transmit) and a multi beam-forming network (to produce number of beams simultaneously in elevation during receive) along with associated electronics.

Simultaneous multi beam formation from an array, which provides enormous data for the radar, plays an important role in height finding radar. The illuminated coverage area in elevation is divided into multiple beams in receive mode and the height of the target is designated with the return of target echo from received beam. Though there exists several conventional method for producing fixed multiple beams, generating simultaneous non-orthogonal multiple beams of varying beam widths with very low side lobe levels has distinct advantages. Design and development of a multi beam antenna (MBA) present several challenges to the antenna designer. A comprehensive computer aided design approach to realize an Ultra Low Side Lobe Multi Beam Triplate Dipole Array Antenna System for Long Range 3-D Surveillance Radar has been developed[27–35]. The aim has been to develop a very systematic &

Figure 11: Horizontally polarized slotted waveguide array antenna for Maritime Patrol radar.

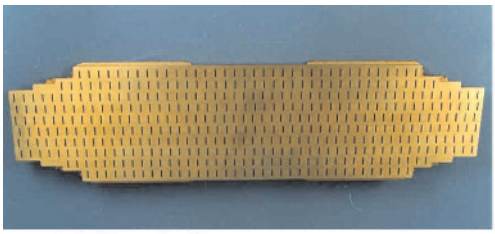

(a) Front view

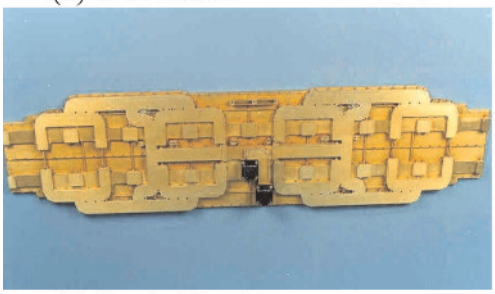

(b) Backside view

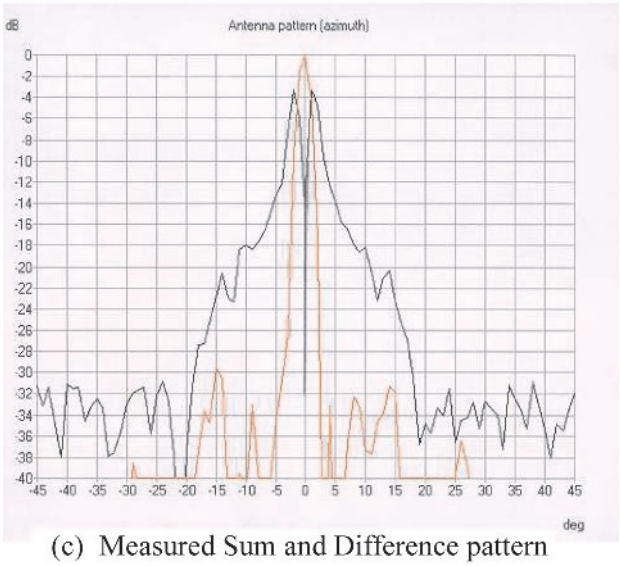

(c) Measured Sum and Difference pattern

comprehensive design methodology in realizing the multi beam antenna system for improved performance with optimum size, weight, volume and performance. The design methodologies and test results of the core elements of the antenna system is presented.

2.3.1. *Ultra low side lobe triplate dipole array*

The 4m long linear array using air-dielectric strip line feed network integrated with 48 triplate dipoles as radiating element has been realized using a computer aided design making an extensive use of commercial 2-D & 3-D softwares. The realization of an ultra low side lobe linear array of 4 m length consisting of 48 triplate dipoles as radiating elements fed by air dielectric stripline power divider network requires design of power dividers with very large power division ratios. The design of such power divided network is intricate as line width becomes extremely small and fabrication is extremely difficult. Special design methods and unsymmetrical topology of feed network design has been evolved to achieve the aim of realizing an antenna with low SLL. The whole network is a combination of sub networks, consisting of T-junctions and modified hybrid ring power dividers. Sub network concept has been resorted to optimize the amplitude and phase at

Figure 12: Circular two plane monopulse array antenna in Ku-band for Missile Seeker Radar applications.

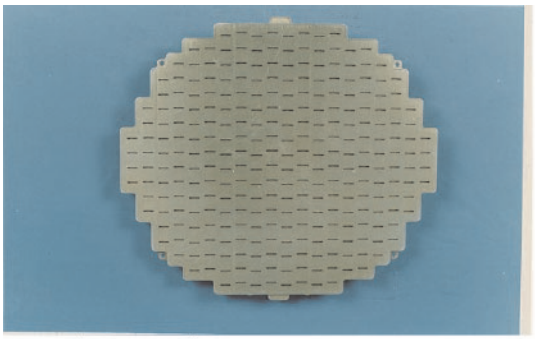

(a) Front view

(b) Backside view

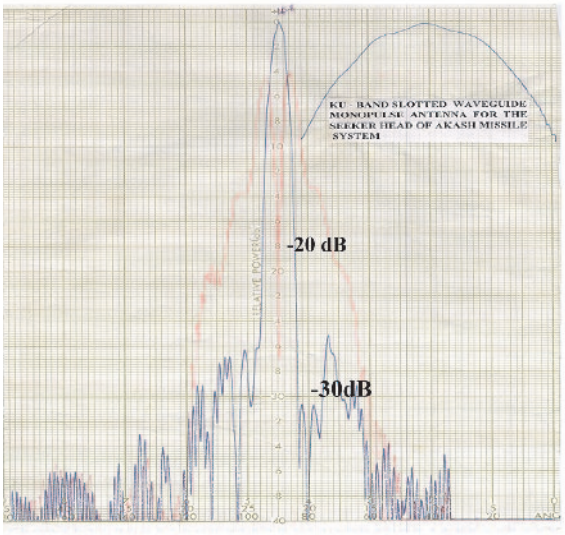

(c) Measured Sum and difference pattern

each hierarchical level to achieve highest degree of amplitude and phase accuracy. It is critical that the center conductor be positioned exactly in the middle of the ground planes with no undulations. Teflon supports, which were used as support for the stripline, and all mechanical tolerances have been taken into consideration in design for efficient manufacture. 32 nos. of such linear arrays are used to make a planar array of size 1.6 m by 4 m. Suitable radome has been developed for environmental sealing of the planar array.

The antenna element is designed and optimized

Figure 13: Non-resonant slotted waveguide array antenna.

(a) Photograph

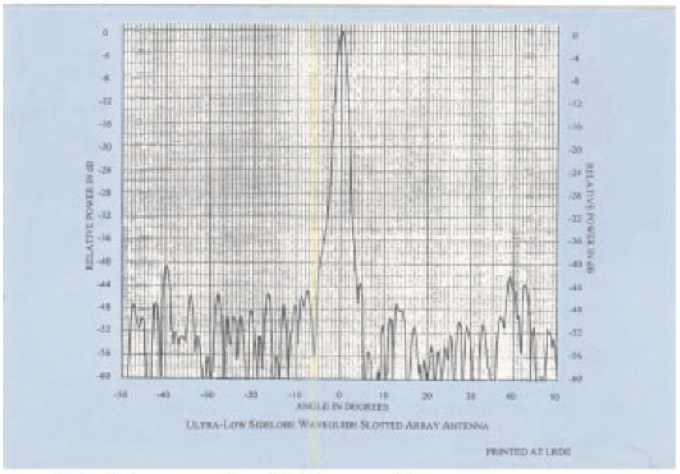

(b) Measured radiation patterns

in the array environment to give the best results. The antenna array is designed to have peak power handling capability of more than 15 KW with a very low peak sidelobe level of the order of −35 dB or less for a very wide band of operation (600 MHz) in S-band. The array has been fabricated using precision machining and EDM wire cutting technologies to achieve the tolerances. View of fabricated air-dielectric stripline power divider network is shwon in Figures 15 and 16 shows fabricated triplate dipole linear array. The array has been tested in near field test range and a typical side lobe performance has been shown Figure 17.

2.3.2. *High power shaped beam forming network*

Shaped beam former generates amplitude and phase which when fed to the planar array forms a cosec-squared pattern. A suitable phase distribution is synthesized and superimposed on the amplitude distribution to generate cosecant-squared pattern. The feeder network is based on wave-guide H plane tee junction with additional septum for fine amplitude control. Since for large amplitude taper distribution and or when number of antenna elements are less the power division ratio to be handled by a single power divider is quite large which leads to narrow bandwidth of operation. To enhance the bandwidth a novel design has been evolved where in an additional septum has been introduced in the broad guide. This innovative power divider will give more than 20% impedance bandwidth for any power division ratio. For high power division ratio, single septum power divider, with its longer length, has a disadvantage. This leads to the risk of arcing due to the proximity to the narrow wall. The additional septum power divider due to reduced length minimizes or virtually eliminates the arcing. The compact, light weight, high power shaped beam antenna feed network based on non-standard, reduced height waveguide

Figure 14: Schematic of a multi beam antenna system.

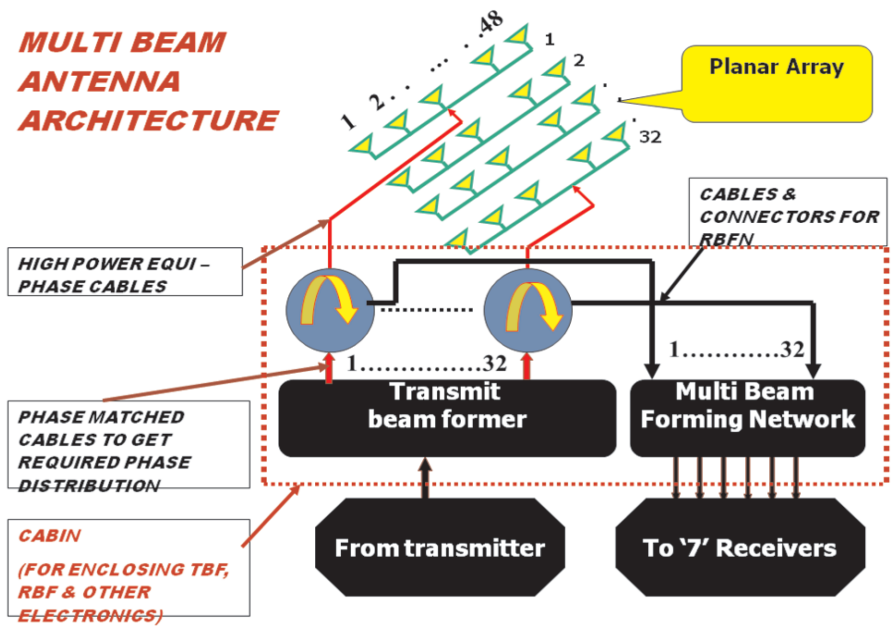

Figure 15: View of fabricated air dielectric stripline corporate power divider network.

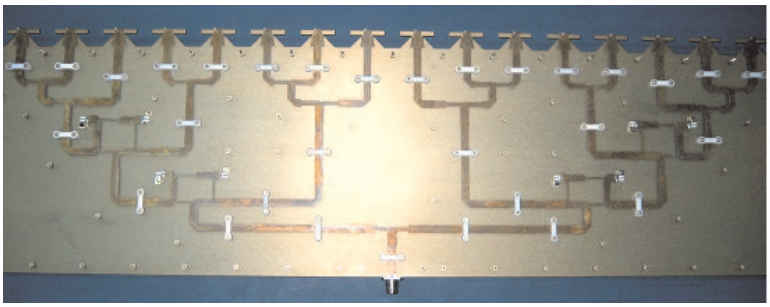

unequal power divider network, with integrated high power cables has been designed, fabricated and evaluated. The entire beam former is realized by machining the waveguide channels from a single aluminium block as shown in Figure 18. A suitable waveguide to co-axial probe has been designed and integrated with the network for connecting the beam former output to the input of the antenna linear arrays through a phase gradient cable to generate required shape. The measured test results of the beam former integrated with the array antenna is shown in Figure 19. The innovative design technique has improved performance with substantial weight reduction, compared to the conventional beam formers.

2.3.3. *Blass multi beam forming network*

To fulfil the requirement of low side lobes with varying beam widths for different beams, non-orthogonal beams and independency of beam position with change in frequency over a wide band, the modified Blass matrix is most suitable. The Blass matrix in its classical form is created from columns and rows made out of TEM mode propagating co-axial line. The rows and columns are interconnected by directional couplers of different but strictly defined coupling values at their cross over points. The columns and rows are terminated with matched loads. The columns are composed of the main path of the directional couplers connected serially while rows are composed of true time delay

Figure 16: Fabricated triplate dipole arrays.

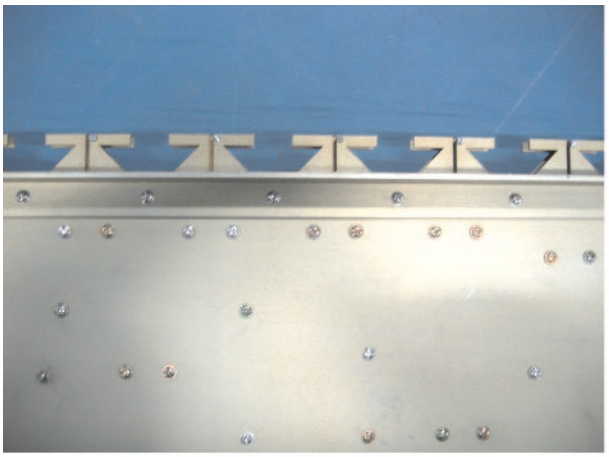

(a) View of a section of dipole linear array

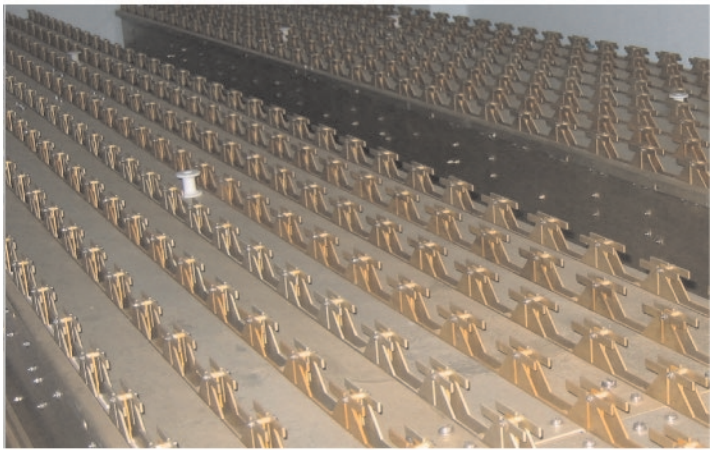

(b) Section of the planar array

lines, auxiliary path of directional coupler and inter column segments. Use of true time delay lines insures the independency of beam position with change in frequency. A signal applied at beam port will progress along the feed line to the end of termination. At each cross over point, a small signal will be coupled into each element line which excites the corresponding radiating element. It may be shown that the field amplitude distribution depends primarily on the coupling coefficients of the directional coupler, whereas the phase distribution depends on the lengths of the inter column segments and true time delay line segments. Different width of the particular beam may be obtained by selecting the number of array elements (rows) activated by given column. This signifies the modification of classical Blass matrix of similar number of rows in all columns (and hence similar beam width for all beams) and hence is called as modified Blass matrix. A schematic of modified Blass matrix is shown in Figure 20.

2.3.3.1. Scattering characteristics of beam forming elements. The main purpose of the synthesis of a beam forming network (BFN) is to get the required parameters of the beam forming elements to achieve the desired complex illumination characteristics of the beam. The performance of the network depends on the scattering characteristics of individual elements used in forming the network. Hence first step necessary to develop a mathematical model for the design of a modified Blass matrix is to choose and understand the behaviour of individual elements. As discussed above, the basic building block of a modified Blass matrix, the selected BFN in the

Figure 17: Measured radiation pattern of the planar array.

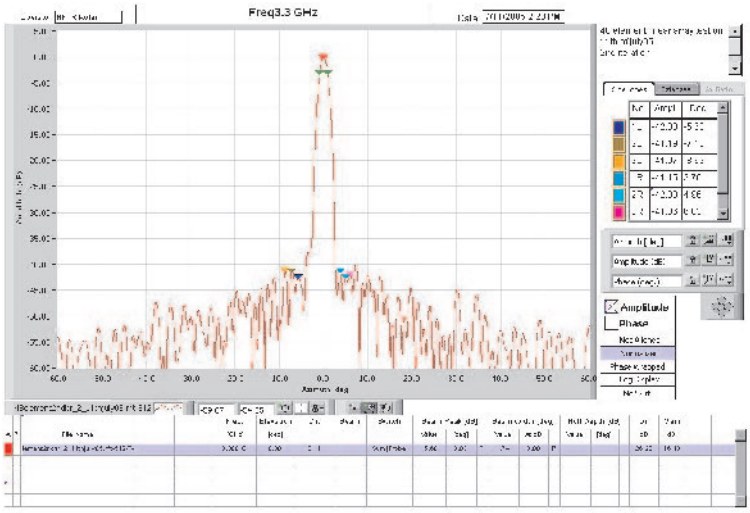

Figure 18: Mechanical views of the shaped beam-former.

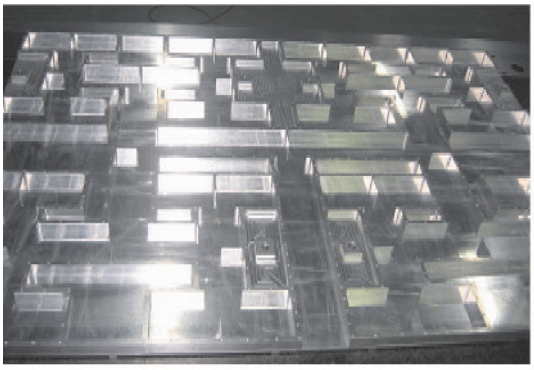

present case, is coupling element, i.e., a directional coupler. Acceptable performance is determined by meeting the impedance and coupling requirements over the required bandwidth. The beam forming network design procedure consists of selecting the appropriate coupling (amplitude) and phase

Figure 19: Measured transmit elevation pattern of the antenna.

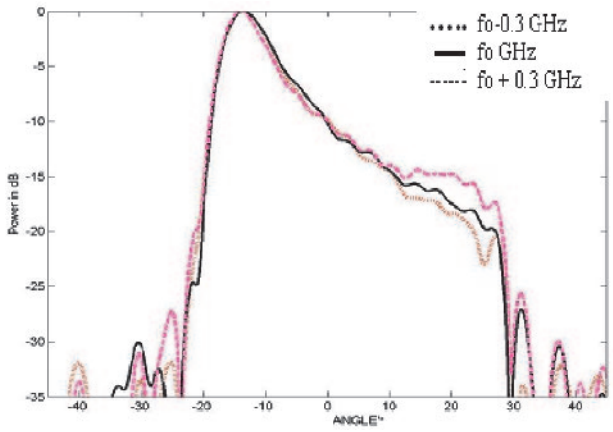

values to achieve the desired beam characteristics. The performance of the network depends on the coupling behaviour of the individual directional couplers used in forming the network. The coupler should furthermore be compact, perfectly matched, have good directivity, allow variable degrees of coupling and should be lossless and reciprocal. Most of the beam former design reported in the literature uses waveguide based couplers called Moreno waveguide cross guide slot coupler. But with this type of couplers, it is very difficult to implement time delay lines with inherent structural complexity. Some of the beam formers have used stripline based directional couplers which has a narrow bandwidth and more loss. The proposed airline directional coupler has shown a wide bandwidth and less loss compared to the couplers described earlier. This type of directional coupler is a coupled slab line of circular cross section enclosed in a rectangular box and named as cylindrical air line directional coupler (Figure 21). The four port coupler which couple energy from mainline to branch line is quarter wavelength long and is symmetrical in nature

Taking into account, the attenuation and phase shift between chosen pair of its ports, the phase difference between real coupler ports can be written as

$$\Psi_{1-2} = \pi/2 - k_1 f; \Psi_{1-3} = -\beta d_g \qquad (47)$$

$$\Psi_{4-3} = \pi/2 - k_2 f; \Psi_{4-2} = -\beta d_p \qquad (48)$$

where, $\beta = 2\pi/\lambda$, $\lambda =$ wavelength in free space, $f =$ frequency; d_g and $d_p =$ length of the mainline and branchline of the directional coupler; k_1, $k_2 =$ phase directional coefficients of coupled channel (port 1–2) and auxiliary channel (port 4–3).

In deriving above relations, it has been assumed that all the ports are perfectly match terminated and phase between isolated coupler ports 2–3 and 1–4 are neglected.

The matrix equation of the directional coupler can be written as

$$\bar{B} = \begin{bmatrix} S_{11} & S_{12} & S_{13} & S_{14} \\ S_{21} & S_{22} & S_{23} & S_{24} \\ S_{31} & S_{32} & S_{33} & S_{34} \\ S_{41} & S_{42} & S_{43} & S_{44} \end{bmatrix} * \bar{A} \qquad (49)$$

where

A, B — are wave approaching to and coming from coupler port;

S_{11}, S_{22}, S_{33}, S_{44} — reflection coefficients of the coupler ports;

S_{14}, S_{23}, S_{32}, S_{41} — transmission coefficients between isolated ports

$$S_{12} = S_{21} = jCe^{-jk_1 f}$$
$$S_{13} = S_{31} = \sqrt{(1-C^2)}10^{-0.05(A_g[dB])}e^{-j\beta d_g}$$
$$S_{42} = S_{24} = \sqrt{(1-C^2)}10^{-0.05(A_p[dB])}e^{-j\beta d_p}$$
$$S_{43} = S_{34} = jCe^{-jk_2 f}$$

where, C is coupling coefficient of the directional coupler; A_g(dB), A_p(dB) are the attenuations in the directional coupler main path (Port 1–3) and auxiliary path (port 2–4). Because of the flow of the signals through cascade connected elements in array, the two port transmission matrix T between different coupler ports is very useful. The transmission matrix can be obtained from the scattering matrix S under the condition that ports are matched.

The following directional coupler parameters are necessarily required to be available as a look up table for the modified Blass matrix design:

Figure 20: Schematic of a modified Blass matrix.

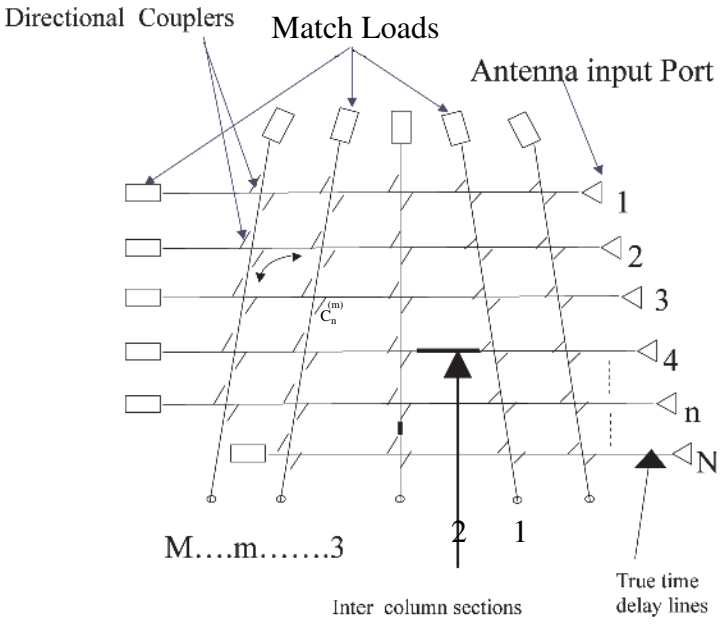

Figure 21: Cylindrical airline directional coupler.

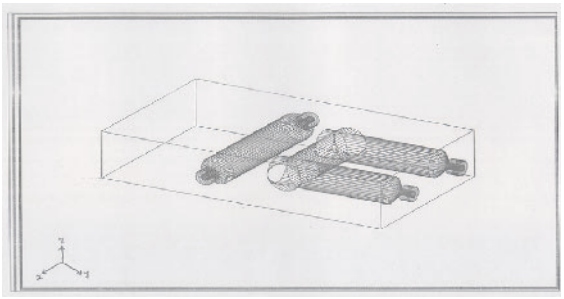

(i) Coupling coefficients of directional coupler over a wide coupling range
(ii) coupler main and auxiliary channel length
(iii) phase directional coefficients for coupled and auxiliary channels
(iv) attenuation in main and auxiliary channels

2.3.3.2. Scattering matrix of the blass array. For the Blass array made out of passive and reversible elements, the reciprocity principle can be applied. Transmission coefficient between source ports and beam ports, independent of the direction of signal flow (transmission or reception), would, therefore, be similar. It is worth to mention that during transmission, if the isolation between coupler ports 1 and 4 are assumed to be infinitely large, the presence of N-row ports terminated into loads can be neglected. On the other hand, during reception, because of the large isolation between coupler ports 2 and 3, M column ports terminated into loads can be neglected. Since $N \gg M$, for all practical applications, it will be easier to operate matrix during transmission. Because of this assumption, the matrix size can be reduced to $N+2M$ instead of $2N+2M$. The assumption of the large isolation between coupler ports is required to be practically ensured to a close approximation. The generalized form of the Blass matrix, taking into account above assumptions, may be presented by the relation (see eqn. (50)). Where, $a_w^{(m)}$, $b_w^{(m)}$ are complex wave approaching to and coming from beam port

$$\begin{bmatrix} b_w^{(1)} \\ \vdots \\ b_w^{(M)} \\ b_1 \\ \vdots \\ b_N \\ b_0^{(1)} \\ \vdots \\ b_0^{(m)} \end{bmatrix} \begin{bmatrix} i=1, j=1 & & j=M & j=M+1 & j=M+N & j=M+2N \\ & S_w^{(m,p)} & & S_n^{(m)} & S_{o,w}^{(m,p)} & \\ i=M & & & & & \\ i=M+1 & & & & & \\ & S_n^{(m)} & & S_{z,k,l} & S_{o,z,n}^{(m)} & \\ i=M+N & & & & & \\ i=M+N+1 & & & & & \\ & S_{o,w}^{(m,p)} & & S_{o,z,n}^{(m)} & S_o^{(m,p)} & \\ i=M+2N & & & & & \end{bmatrix} \begin{bmatrix} a_w^{(1)} \\ a_w^{(M)} \\ a_1 \\ a_N \\ a_0^{(1)} \\ a_0^{(M)} \end{bmatrix} \tag{50}$$

a_n, b_n are complex wave approaching to and coming from source port

$a_0^{(m)}$, $b_0^{(m)}$ are complex wave approaching to and coming from load terminated column port

The expressions of individual sub matrix of the scattering matrix S may be interpreted as follows:

$S_{ij} = S_w^{(m,p)}$ for $i = 1, M$; $j = 1, N$; $i \neq j$

(indicating transmittance between mth and pth beam port)

$S_{ij} = S_n^{(m)}$ for $i = 1, M$; $j = M+1$, $M+N$ or $i = M+1$, $M+N$; $j = 1, M$

(indicating transmittance between mth beam port and nth source port)

$S_{ij} = S_{o,w}^{(m,p)}$ for $i = 1, M$; $j = M+N+1$, $M+2N$ or $i = M+N+1$, $M+2N$; $j = 1, M$

(indicating transmittance between mth beam port and load terminated pth column port)

$S_{ij} = S_o^{(m,p)}$ for $i = M+N+1$, $M+2N$; $j = M+N+1$, $M+2N$; $i \neq j$

(indicating transmittance between load terminated mth and pth column port)

$S_{ij} = S_{o,z,n}^{(m)}$ for $i = M+1, M+N$; $j = M+N+1$, $M+2N$ or $i = M+N+1$, $M+2N$; $j = M+1, M+N$

(indicating transmittance between nth source port and load terminated mth column port)

$S_{ij} = S_{z,k,l}$ for $i = M+1, M+N$; $j = M+1$, $M+N$; $i \neq j$

(Indicating transmittance between kth and lth source ports)

$S_{ij} = \Gamma_{ii}$ $(i = j)$: reflection coefficient

2.3.3.3. Determination of beam forming scattering matrix. For the synthesis of beam forming system, it is essential to know the specified transmittance S_{ij} of the Blass array scattering matrix. This is determined by analysing the signal path between beam port and source port as well as beam port and load terminated column port. From the analysis, it results that the signal between these ports, from second channel onward, run in large number of various paths. The number of various signal path increases with the number of channels.

Generally, there exists two type of signals namely primary signal (I_p) and additional signal (I_d). The primary signals (also called first order signals) on their path in beam forming network are decoupled in directional coupler only once while additional signals may be decoupled two, three or number of times (called 2nd, 3rd or nth order signal). The additional signal also includes the zero order signal i.e., the signal which is not decoupled and is proceeding along given column. It has been found out that only odd signal contribute to the beam formation.

2.3.3.4. Determination of coupling coefficient of directional couplers. To determine the coupling coefficient of directional coupler, it has been assumed that

(i) the resultant wave reflecting from the nth source corresponds to the specified field distribution $I_{no}^{(m)}$ for the mth channel

(ii) the wave $a_w^{(m)}$ coming to the mth beam port has a value of unity.

Taking above assumptions into account, the coupling coefficient of the nth coupler in the first channel has been derived and is given by

$$C_n^{(1)} = \frac{-j\sqrt{\eta^{(1)}} I_{n0}^{(1)} K^{-1}[\alpha^{(1)} l_n^{(1)}] \psi^{-1}[\beta \sqrt{\varepsilon_r^{(1)}} l_n^{(1)}}{\sqrt{\sum_{n=N_d^{(1)}}^{N} I_n^{(1)^2} \prod_{t=N_d^{(1)}}^{n-1} \sqrt{1 - C_t^{(1)^2}}} K[(n-1)A_g] \psi[\beta(n-1)d_g, -(k_1 f)]} \tag{51}$$

wherein

$$I_{n0}^{(1)} = I_{n0}^{(1)} e^{j\phi_{n0}^{(1)}} \tag{52}$$

$$\eta^{(1)} = \frac{\sum_{n=N_d^{(1)}}^{N} I_{n0}^{(1)} I_{n0}^{1*}}{I_w^1 I_w^{1*}} \tag{53}$$

where

$I_{n0}^{(m)}$, and $\phi_{n0}^{(m)}$ assumed field distribution of the m-th channel corresponding for amplitude and phase

$\eta^{(m)}$ — energy efficiency of the m-th channel

$I_w^{(m)}$ — signal on the input port of m-th beam, assumed equal to unity.

In the case of channel $m \geq 2$, for which the field distribution at the source is the superposition of the primary signal and additional series of signals, the expression for the coupling coefficient is found to be

$$C_n^{(m)} = \frac{-j\sqrt{\eta^{(m)}} I_{n0}^{(m)} K^{-1}(\alpha l_n^{(1)}) \psi(\beta\sqrt{\varepsilon_r} l_n^{(1)}) + \sqrt{\sum_{n=N_d^{(m)}}^{N^{(m)}} I_n^{(m)^2} \sum_{p=1}^{n-1} R_{m,n}^{p}}}{\sqrt{\sum_{n=N_d^{(m)}}^{N^{(m)}} I_n^{(m)^2} \prod_{t=1}^{m-1} \sqrt{1-C_n^{(t)^2}} \prod_{t=N_d^{(m)}}^{n-1} \sqrt{1-C_t^{(m)^2}} K[(n-N_d^{(m)})A_g, \alpha \sum_{t=2}^{m} l_n^{(t)}, (m-1)A_p]}}$$
$$\psi^{-1}\{\beta[(n-N_d^{(m)}) d_g \sqrt{\varepsilon_r^{(1)}} \sum_{t=2}^{m} l_n^{(t)}, (m-1)d_p], k_1 f\} \tag{54}$$

wherein

$$\eta^{(m)} = \frac{\sum_{n=N_d^{(m)}}^{N^{(m)}} I_{n0}^{(m)} I_{n0}^{(m)*}}{I_w^{(m)} I_w^{(m)*}} \tag{55}$$

$$I_{n0}^{(m)} = I_{n0}^{(m)} e^{j\phi_{n0}^{(m)}} \tag{56}$$

$$\begin{aligned} R_{m,n}^{(p)} = {} & C_n^{(p)} \prod_{t=1}^{p-1} \sqrt{1-C_n^{(t)^2}} K\left[\sum_{t=1}^{p-1} A_{p,n}^{(t)}, \sum_{t=2}^{p} \alpha^{(t)} l_n^{(t)}\right] * \\ & \psi\left\{\beta\left[\sum_{t=1}^{p-1} d_{p,n}^{(t)}, \sum_{t=2}^{p} \sqrt{\varepsilon_r^{(t)}} l_n^{(t)}\right], k_{1,n}^{(p)} f\right\} \sum_{k=N_d^{(m)}}^{n-1} C_k^{(m)} C_k^{(p)} * \\ & \prod_{t=p+1}^{m-1} \sqrt{1-C_k^{(t)^2}} \prod_{t=N_d^{(m)}}^{k-1} \sqrt{1-C_t^{(m)^2}} \prod_{t=k+1}^{n-1} \sqrt{1-C_t^{(p)^2}} K \\ & \times\left[\sum_{t=N_d^{(m)}}^{k-1} A_{g,t}^{(m)}, \sum_{t=k+1}^{n-1} A_{g,t}^{(p)},\right] * K\left[\sum_{t=p+1}^{m} \alpha^{(t)} l_t^t \sum_{t=p+1}^{m-1} A_{p,k}^{(u)}\right] \\ & \times\psi\left\{\beta\left[\sum_{t=N_d^{(m)}}^{k-1} d_{g,t}^{(m)}, \sum_{t=k+1}^{n-1} d_{g,t}^{(p)},\right], \sum_{t=p+1}^{m} \sqrt{\varepsilon_r^{(t)}} l_k^{(t)} * \right. \\ & \left. \sum_{t=p+1}^{m-1} d_{p,k}^{(t)}, k_{1,k}^{(m)} f, k_{2,k}^{(p)} f\right\} \end{aligned} \tag{57}$$

In the case of first channel for which the distribution is formed only through primary signal, the phase of coupling coefficient does not depend on the source number n while for other channels it varies with n.

Since above equations are recurrence equations, to get any arbitrary value of coupling coefficients $C_n^{(1)}$ or $C_n^{(m)}$ it is required to know all the values which they precede. This means it is required to proceed step by step, i.e., from the determination of coupling $C_n^{(1)}$ for $n = 1$ in the first channel upto the determination of coupling of the last coupler $C_N^{(M)}$ (for $n = N$ in M^{th} channel).

2.3.3.5. Features of antenna systems developed. Using above expressions the multi beam forming network is designed & developed to generate 7/8/9 low side lobe beams of different beam width in pre fixed position in elevation plane during receive for different applications. It uses 7/8/9 channels of air-line cylindrical directional coupler integrated as a modified Blass matrix with inter connecting true delay lines to form 7/8/9 beams at the specific beam pointing location. The photograph of a 7 channel beam forming network is shown in Fig. 22. Rigorous evaluation of the feed network has been carried out and the results are shown in Fig. 23. A Peak side lobe level better than –30 dB and beam pointing accuracy less than 0.1 degrees over a band of 500 MHz has been obtained.

Significant Features of Rohini Antenna (Figure 24)

Planar Array consisting of 32 linear triplate dipole

array of size 4 meters

1 : 32 Shaped beam forming network to produce shaped beam to cover elevation upto 40 degrees

32×7 Blass Network to produce 7 beams

Side Lobe Level : < -35 dB (Peak), -45 dB (rms)

Significant Features of Revathi Antenna (Figure 25)

Planar Array consisting of 24 linear triplate dipole array of size 4 meters

1 : 24 Shaped beam forming network to produce shaped beam to cover elevation upto 50 degrees

24×8 Blass Network to produce 8 beams

Side Lobe Level : < -35 dB (Peak), -45 dB (rms)

3. Electronic scanning arrays

Electronic scanning arrays differ from conventional mechanically scanned arrays in two fundamental aspects — it is mounted in a fixed position on the platform and its beam is steered individually by controlling the phase of the radio waves

Figure 22: Photographs of multi beam forming network.

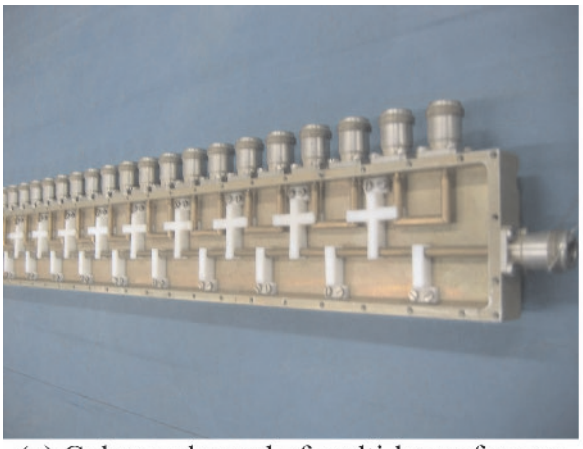

(a) Column channel of multi-beam former

(a) Assembled beam-forming network

transmitted and received by each radiating elements. Electronically scanned arrays offer many advantages to the radar system designer such as agile beams, low profile and scalability. There are two types of electrically scanned arrays; passive phased arrays and active phased arrays. Passive phased arrays have central transmitter and receiver, with phase shifters located at each radiating element or sub array. Active phased arrays use transmit/receive modules (TRMs) to provide the last stage of amplification for transmitted signal, the first stage of amplification for received signals, and provide both amplitude and phase control at each radiating element. During the last two decades, LRDE has developed state-of-the-art phased array radar systems based on the passive & active phased arrays technologies developed in the country.

3.1. *Passive phased arrays*

A phased array antenna[5,39–41] composed of a number of radiating elements each with a phase shifter. Radiations from these elements constructively or destructively interfere to result in the final beam which is controlled by the phase if the signal radiated from these elements.

For example, when all radiating elements are fed with the same phase, the emitted signals add up by constructive interference in the main (boresight) direction. But if the signals in consecutive elements are shifted by a progressive phase shift, the main direction of the emitted sum-signal is moved away from the boresight direction. The main beam always points in the direction of the increasing phase shift. Thus if the inputs to radiating elements are delivered through an electronic phase shifter giving a continuous phase shift now, the beam direction will be electronically adjustable.

Figure 23: Measured radiation pattern in elevation plane. Formation of seven simultaneous beams is shown here.

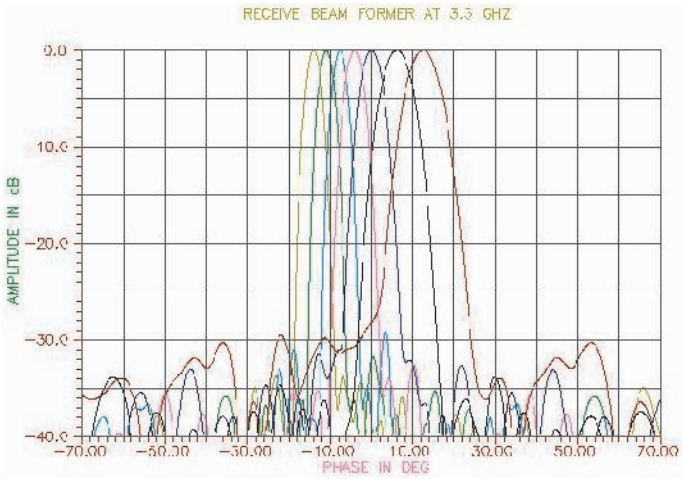

Figure 24: Photograph of Rohini (IAF) radar.

Phased array antennas can be used to impart directional capabilities to radars and modern communication systems. A phased array includes a set of antennas (called an array), a feed network, a set of phase shifters and their control circuits. As the number of elements in the array increases, such a system tends to occupy a large space. These elements are arranged as linear, circular or planar arrays based on beam shaping requirements.

Linear array antennas consist of lines whose elements are fed about a common phase shifter. This is a simple arrangement, but can scan the beam only in one plane. This kind of the phased-array antenna is commonly used as in many applications this would suffice. On the other hand, planar antenna arrays consist of radiating elements arranged in a plane, each of which having a separate phase shifter. These elements are ordered in a matrix array. This arrangement makes it possible to steer the beam in two planes and is also extendable for digital beamforming networks. However this often has complicated assembly requirements and a large number of electronically controlled phase shifters are needed

The phase increment required between successive element may be calculated easily for a linear array. Assuming isotropic radiators for the moment, for a separation of d between such elements, the scan angle θ_s and phase shift $\Delta\phi$ are related by,

$$d\sin\theta_s = \Delta\phi\lambda/2\pi \qquad (58)$$

Figure 25: Photograph of Revathy (Navy) radar.

where λ is the free space wavelength of the radiation. It may be noted that the phase of each successive element is shifted by $\Delta\phi$. Hence in a typical situation, phase shifters are required have the option to provide full 360° phase shift. A phase shifter is therefore one of the main components for such radar systems with phased arrays. Phase shifter causes a change in the phase of output signal w.r.t. the input signal[41]. Such antenna arrays can replace antennas with conventional large reflectors on mechanical steering arrangements discussed in the previous section. Incidentally, these array antennas can also provide the capability to reduce co-channel interferences, reduction in delay spread, multi-path fading, resulting in better quality of services, such as reduced Bit-Error-Ratio (BER) and outage probability for mobile communications. In the conventional approach the antenna is rotated mechanically to steer the beam (mechanical steering). In contrast, in a phased array, the phase-shift provides the effective rotation of the beam (electronic steering). Obviously, such antenna systems have a faster scan speed. Recent advances in microwave monolithic integrated circuit (MMIC) have made it possible to incorporate high power generation (on transmit) and low noise preamplification (on receive) within the phased array antennas.

Conventional phase shifter circuits can be broadly categorized into analog phase shifters and digital phase shifters. The analog phase shifters can produce continuously varying phase shift ranging from 0 to 360. However in a digital phase shifter the phase change occurs in discrete steps. For example, a 2-bit phase shifter based on 45/90 set of delay networks can generate 0, 45, 90, 135 phase shift depending on the bit combination[41]. Yet these are preferred by the industry due to the easy availability of digital control circuits. Desired characteristics for a phase shifter are:

- Good impedance match
- Sufficient power handling capacity
- Low drive power
- Fast response speed.

Typical advantages of a phased array antenna include

- High gain width los side lobes
- Ability to permit the beam to jump from one target to another in very short time (microseconds typical)
- Ability to provide an agile beam with digital control
- Arbitrarily modes of surveillance and tracking
- Multi-mode/multifunction operation by emitting several beams simultaneously
- The system remains operational even with a faulty element, (with reduced beam sharpness).

Their disadvantages include

- the coverage is limited to a 120 degree sector in azimuth and elevation
- deformation of the beam while the deflection
- low frequency agility
- very complex structure (processor, phase shifters)
- still high costs.

Figure 26: Measured radiation patterns of Rajendra phased array.

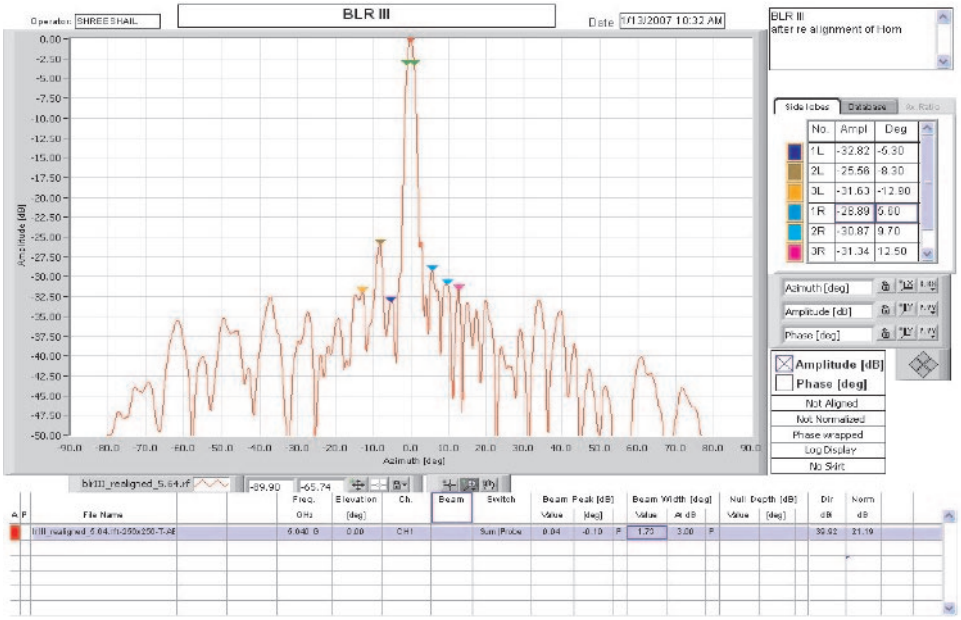

(a) Azimuth plane pattern

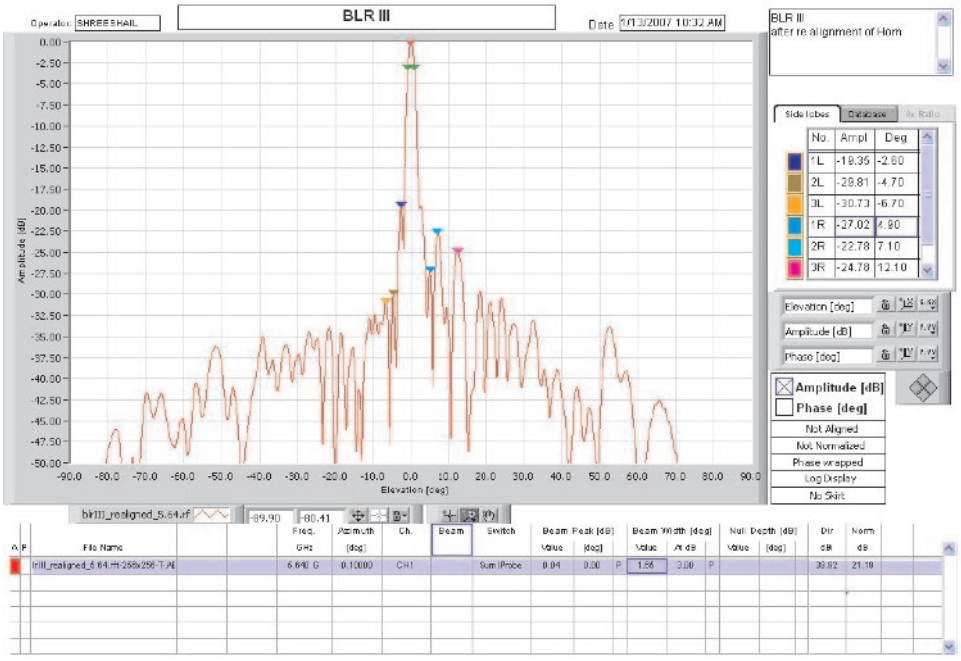

(b) Elevation plane pattern

3.2. *Phased array development at LRDE*

With the rapid changes in Radar scenario, Radar system is required to have high data rates and multifunction capabilities. This necessitated the use of Electronic capability using phased array antenna. Unlike mechanically scanned array antenna system, it has an electronically controlled phased shifter immediately behind each radiating element. Since these phased array antennas are larger in size to meet the requirements of the Radar systems, these arrays are used in "less mode of operation". This requires the integration of (i) Pick-

Figure 27: Rajendra phased array antenna in the deployed condition.

up element (ii) Digital Phase Shifter and (iii) Radiating element all into one module called Phase Control Module (PCM) and also required to be dielectrically loaded to meet the inter element spacing requirements of an array environment. In addition, these electronically scanned antennas are to have monopulse capability to meet the tracking requirements of a "multifunction Radar System". In order to electronically steer the beam, the phase shifters are controlled rapidly through a Beam Steering Computer.

Initially, studies were carried out to check the capabilities of the PCMs in the array environment and then to steer the beam to the required position through a Beam Steering unit which lead to the maturity in the Design and Development of a phased array antenna. Also this required a quantum jump in the feed technology to have two dimensional monopulse capabilities.

The monopulse feed horn developed is based on the use of multimodes to generate sum and two difference signals. The sum signals uses the TE10 mode, the TE20 modes and (TE11 + TM11) modes generate the azimuth and elevation difference signals respectively.

Such a "phased array antenna" with two phase monopulse capability" has been implemented successfully for Rajendra phased array radar for Akash surface to air missile system and Weapon Locating Radar.

Rajendra phased array radar uses about 4000 phase control modules operating in C-band to provide an electronic scanning of the beam in all the directions to an extent of ± 50 degrees. A representative plot showing the side lobe performance of the Rajendra phased array after carrying out the necessary array collimation in planar near field test range is shown in Figure 26. Figure 27 shows Rajendra Phased Array radar.

Weapon locating radar is a derivative of Rajendra radar to detect and track artillery shells and predict the location of the gun, weapon, artillery etc which is not in the line of sight. The phased array uses about 6000 PCMs arranged in triangular lattice to provide the required beam characteristics. A photograph of the phased array mounted in near field test range for carrying out necessary collimation and generating the phase look up table for each beam scanned in different directions is shown in Figure 28. A typical azimuth and elevation plane patterns of the array are shown in Figure 29.

3.3. *Active aperture antenna system*

During the last few years LRDE has been concentrating in developing active array technology based radar systems. Towards this, lot of efforts has been put into the development of indigenous transmit / receive modules, the most critical and important module of an active array antenna system.

To develop antenna system with emerging technologies such as T/R module based active aperture with electronically steerable multi beam technology indigenously was a challenge. The development of S-band T/R modules of requisite power, one of the most critical component of the active aperture radar, configuration of the active array radar with indigenously developed T/R modules and their thermal management, functional requirement and techniques of active aperture calibration & diagnostic was very critical because of

Figure 28: Measured radiation patterns of WLR phased array.

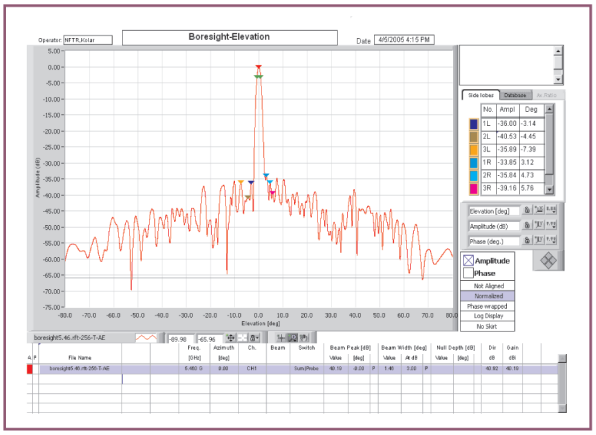

(a) Azimuth plane pattern

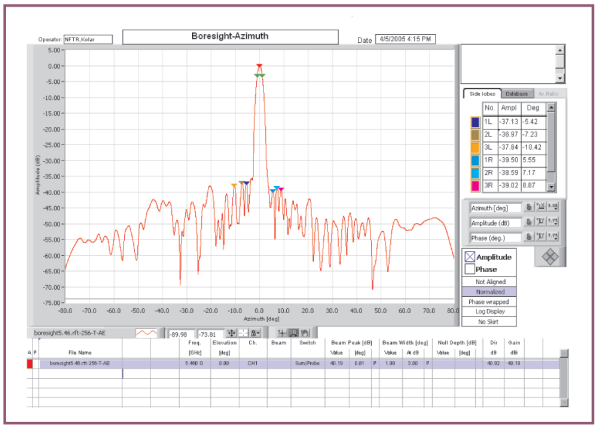

(b) Elevation plane pattern

the complexity involved in the technology. Further, this being a active array with cosecant squared shaped beam during transmit and multiple pencil beams during receive in elevation with elevation beam tilt facility electronically, a systematic process has been developed to carry out the active array calibration and collimation in automated planar array antenna near field test range. The calibration of an active array radar system is of utmost importance because all the requisite amplitude and phase data of the T/R modules for different beams at different tilt angles and at all the radar frequency operation spots for different temperature ranges need to be measured and stored as look up tables in the beam steering controller residing in radar controller. As the calibration of an active array radar system is of utmost importance, establishing the calibration process is going to be a mile stone for all the (present & future) active aperture radar development in the country.

A high performance semi distributed active array antenna technology has been realized cost effectively meeting stringent functional, mechanical, environmental and EMI/EMC requirements. Core competency in the following critical areas has been established:

1. Realization of a very low side lobe linear arrays of 1.5 m length consisting of 18 radiating elements integrated with power divider network. A design and manufacturing methodology for achieving a very low peak SLL, a good input match using indigenously developed non-standard waveguides has been established. The manufactured array has shown a peak SLL better than –30 dB with a very good input VSWR.

Figure 29: Photographs of weapon locating radar.

(a) Array mounted in near field test range

(b) Array in deployed condition

2. Development of 20 W, 65 W and 100 W T/R modules in S-band and their thermal management along with associated electronics and controllers within the specified weight budget was the most complex job and the same has been done successfully.
3. Realization of Transmit, bite & calibration networks using microstrip circuits. This innovative design has benefited enormously in improving the performance, reducing the volume and weight.
4. Realization of very light weight, high performance multi beam forming network using modified Blass matrix to generate multiple low side lobe beams in elevation at pre-fixed elevation angles with no deviation in beam positions with frequency in the required band of operation.
5. Establishing Transmit / Receive module test procedure in transmit (pulsed operation) & Receive modes.
6. Establishing TRM calibration (both in Transmit as well as receive) using Vector Network Analyzer.
7. Establishing Active Array Calibration and collimation test procedures in Antenna Near Field Test Range.
8. Implementation of mitigation techniques for T/R module failure.

The technology has been successfully implemented in developing the first active aperture radar named ASLESHA for low level surveillance in mountainous terrain and high altitude regions. Azimuth and elevation patterns of the active array antenna system alongwith electronically steerable coverage diagram produced by the antenna is shown in Figure 30. Photograph of Aslesha in deplyed condition is shown in figure 31.

Figure 30: Radiation patterns of Aslesha radar antenna.

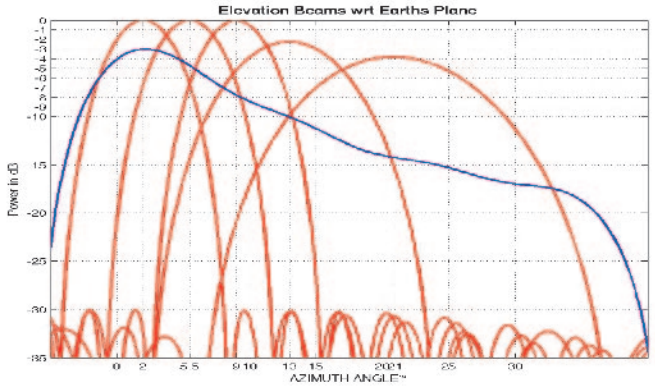

(a) Elevation Beam patterns (Blue –Tx pattern, Red: multiple Rx patterns)

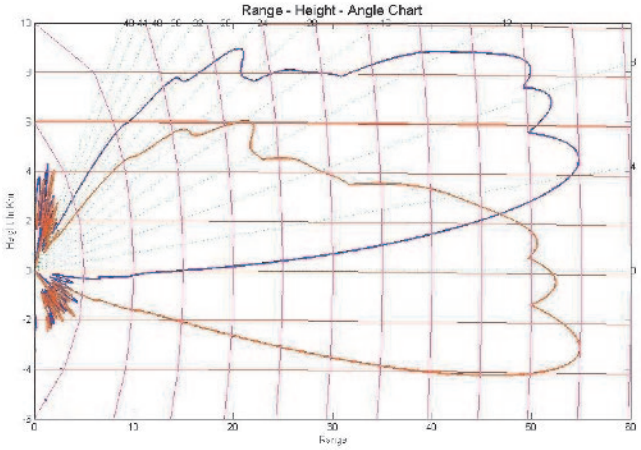

(b) Electronically steerable radar coverage diagram

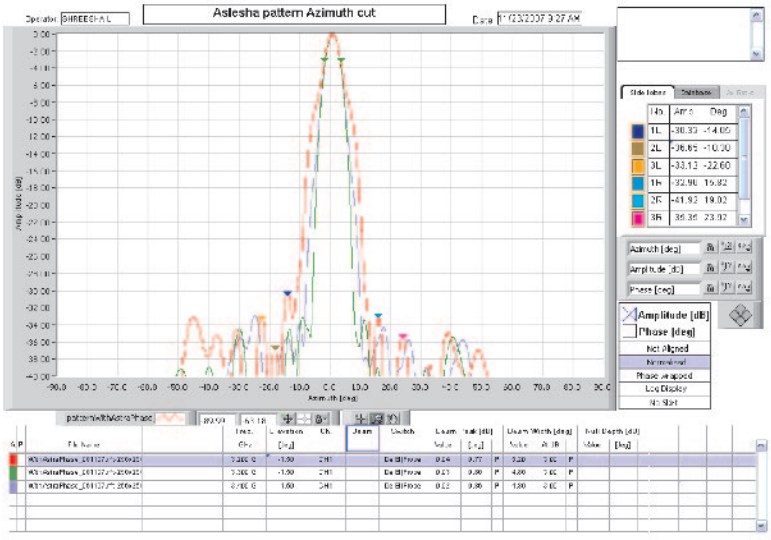

(c) Measured azimuth beam patterns

Figure 31: Photograph ofAslesh semi-distributed active antenna system.

3.4. *Active array antenna system with digital beam forming*

The advances provided by Moore's law has now made it feasible to do digital beam forming with all its numerous advantages. One advantage of DBF is the ability to lower the search power and occupancy by upto a factor of two. Another advantage is that it makes its possible to achieve the performance of a fully adaptive array without having to do a large matrix inversion.

In beam forming, both the amplitude and phase of each antenna element are controlled. Combined amplitude and phase control can be used to adjust side lobe levels and steer nulls better than can be achieved by phase control alone. The combined relative amplitude $\mathbf{a}_k$ and phase shift θ_k for each antenna is called a "*complex weight*" and is represented by a complex coefficient $\mathbf{w}_k$(for the kth element of antenna). In analog beam forming the operation of phase shifting and amplitude control is done with the help of phase shifters and passive beam formers.

But in digital beam forming, the operations of phase shifting and amplitude scaling for each antenna element, and summation for receiving, are done digitally. Digital processing requires that the signal from each antenna element is digitized using an A/D converter. Since signals at RF frequencies ($>$30 MHz) are too high to be directly digitized at a reasonable cost, digital beam forming receivers use analog "RF down /upcoverters" to shift the signal frequency down before the A/D converters.

Once the antenna signals have been digitized, they are passed to "digital down-converters" that shift the signal center frequency down to 0 Hz and pass only the bandwidth required for one channel. The down-converters produce a "quadrature" baseband output at a low sample rate.

Each the quadrature baseband Q components and I are then multiplied by complex weights required and the results are summed to produce one baseband signal for forming the beam in particular direction.

Digital Beam Forming Radar has the following characteristics

1. Closely spaced stacked beams without degradation in signal to noise ratio.
2. Adaptive null steering. This is possible due to the precise and predictable nature of the weighting operation in a digital processor, which allows the best and most rapid control of beam shape.
3. The gain and phase errors in all the receiver channels are maintained within acceptable tolerance limits or can be compensated. This allows ease of receiver calibration.

Figure 32: Typical block diagrams showing digital beam forming processing.

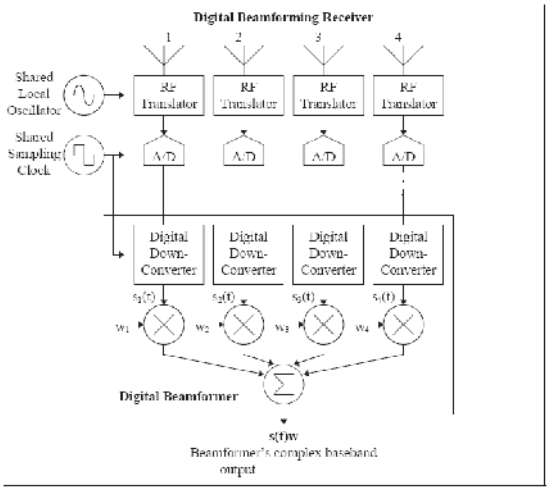

(a)

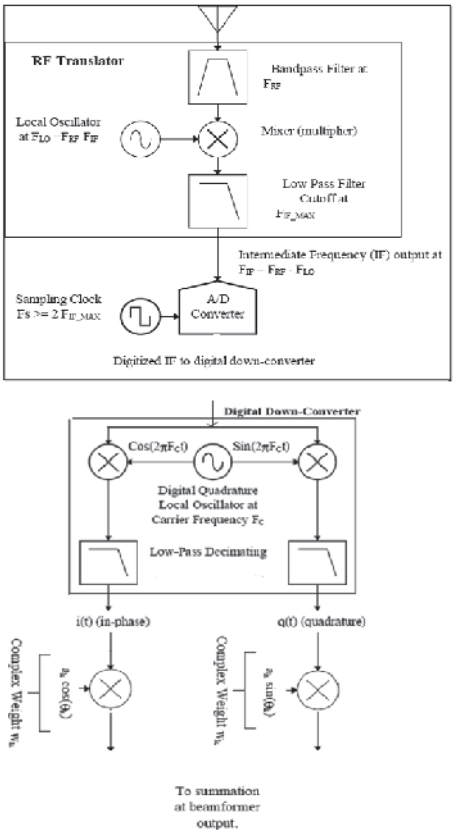

(b)

4. Due to maintenance of gain and phase errors in the receiver channels within acceptable tolerances, realization of ultra low side lobes are possible.

Block diagram of a DBF array and its processing is shown in Figure 32.

4. Summary

A number of antenna systems developed in recent decades for challenging radar applications by the defense research and development organization are discussed in this review paper. These include mechanically steered antenna systems such as

doubly curved reflector antenna systems for Indian pulse doppler radar (INDRA) and low level light weight radar (Bharani) for army air defence, slotted waveguide array antenna for fire control radar of light combat aircraft (LCA) and for maritime patrol radar (for Indian navy and Polish defence), and battle field surveillance radar.

Another development was the multi beam antenna system for medium range 3D surveillance radar for air force (Rohini), navy (Revathi) and tactical control radar (TCR) for army. These antenna use beam forming networks, the design of which are also included in this article. In addition, several phased array radars have also been designed and developed. These include Rajendra for Akash SAM for air force and army, and those for weapon locating radar (WLR). Features of a recently developed semi distributed active aperture antenna for 3D low level surveillance radar Aslesha is also discussed in this context. The development of digital array based 4D radar systems for long range surveillance radar is currently under developmental process and it may take two to three years before it becomes the reality in India.

5. Acknowledgment

The author would like to thank Shri S Varadarajan, Outstanding Scientist & Director, LRDE, DRDO, Bangalore and Dr D C Pande, Divisional Officer, C-Radar Division for their fruitful discussion and encouragement to establish critical antenna technologies in LRDE and their permission to publish the work. Author would also like to thank colleagues from LRDE including Shri U S Pande, Mrs Shubha Elizabeth, Dr I A Khan, Ms Preeti for sharing lot of information in preparing the manuscript.

Received 2 June 2010; revised 26 October 2010.

References

1. IEEE Transactions on Antennas and Propagation, Vols AP-17, No.3, May 1969, AP-22, No. 1, Jan 1974; and AP-31, No. 6, Part II, 1983
2. Constantine A. Balanis, Antenna Theory : Analysis and Design, 3rd edition, 2005, John Wiley & Sons, Inc.
3. Proceedings of the IEEE, Vol. 80, No. 1, January 1992
4. Merrill I. Skolnik, Introduction to Radar Systems, Tata McGraw-Hill, 2005
5. Merrill I. Skolnik, Radar Handbook, McGraw-Hill, 2/e, 1990, pp. 6.30-6.33.
6. S. Silver, Microwave Antenna Theory & Design, New McGraw-Hill,1949, pp. 502–508.
7. Thomas F. Carberry, Analysis Theory for the Shaped-Beam Doubly Curved Reflector Antenna, IEEE Trans. Antenna and Propagation, Vol. AP-17, No.2, March 1969, pp. 131–138.
8. Anton Brunner, Possibilities of Dimensioning Doubly Curved Reflectors for Azimuth-Search Radar Antennas, IEEE Trans. Antenna and Propagation, Vol. AP-19, No.1, January 1971, pp. 52–57.
9. Shivaram A. N. *et al.*, Design of Aperture Limited Doubly Curved Reflector Antenna, Proc. ICAT-2009, Ahamadabad
10. Elliot R. S., Antenna Theory and Design, Englewood Cliffs, NJ, Prentics Hall, 1981
11. Sparks R. A., Syatem applications of Mechanically scanned array antennas, Microwve J. 31 (June 1988), pp. 26–48
12. Evans G. E. and H. E. Schrank, Low side lobe radar antennas, Microwave J. 26 (July 1983), pp. 109–117
13. A. F. Stevension, Theory of slots in rectangular waveguides, J. Appl. Phys., Vol. 19, pp 24–38, 1948
14. S. R. Rengarajan, Compound radiating slots in the broad wall of a rectangular waveguide, IEEE-AP, Vol. 37, pp. 1116–1123, 1989.
15. R. F. Harrington, Field computation by method of moments, McGraw-Hill, New York, 1969.
16. S. Christopher, A. Kaul and VVS Prakash, Characterization of Broad wall Radiating Slots -CoBRa, Registration No. L-14429/95 (India)
17. S. Christopher, V.V.S. Prakash, A. K. Singh & N. Balakrishnan, Moment Method analysis of dielectric covered radiating slots using alternative Green's function approach, Proc. Applied Computational Electromagnetics, 1995, pp 680–686, USA
18. S. Christopher *et al.*, Characterization of Dielectric Covered Broad wall Radiating Slots –CoBRa-DC, Registration No. L-/95 (India)
19. A. K. Singh and S.Christopher, Scattering characteristics of dissimilar waveguide slot couplers, Proc. Applied Computational Electromagnetics, pp. 664–671, 1995, USA.
20. S. Christopher and A.K. Singh, Characterisation of broad wall inclined coupling slots – CoBICS, Registration No. L-16186/97, India
21. A. K. Singh, S. Christopher and K. U. Limaye, Moment method analysis of non-orthogonal waveguide to waveguide coupling through slot, Proc. Applied Computational Electromagnetics, pp. 155–162, 1994, USA.
22. A. K. Singh and S.Christopher, Moment method analysis of longitudinal/transverse waveguide slot coupler, Proc. Progress in Electromagnetic Research Symposium, 1997, HongKong
23. S. Christopher, A. K. Singh *et al.*, Design of resonant slotted waveguide planar array for air borne applications, Proc. Asia-Pacific Microwave Symposium (APMC-1995), 1995, Korea.
24. S. Christopher et al,Efficient mutual coupling computations for symmetrical arrays, Proc ACES-1994, USA
25. S. Christopher et al, Design aspects of compact high power multi port unequal power divider, IEEE Int. Symp. on Phased Array System & Technology, Oct. 15–18, 1996, Boston, USA.
26. A. K. Singh & S Christopher, CAD of a compact monopulse comparator network using planar magic tee junctions for slotted array antennas, Microwave J., pp. 110–126, 2001, USA
27. Preeti D., Shubha E. A. & Singh A. K., Design of ultra low sidelobe level linear array for medium range surveillance radar, IEEE – ISM2008, India
28. Preeti D. & A. K. Singh, Design of an ultra low side lobe traveling wave edge slot array, IEEE – ISM2008, India
29. Shubha Elizabeth A. & A. K. Singh, 'Failure mitigation of semi active multi beam antenna array for portable surveillance radar using genetic algorithm, IEEE Radar Conference (RADCON-08), May 26–30th, 2008, Rome, Italy.
30. A. K. Singh, Shubha Elizabeth & Preeti D., Ultra Low Side Lobe Electronically Steerable Multi Beam Antenna System for Long Range 3D Naval Surveillance Radar', IEEE Radar Conference, pp. 457-462, 2007, USA
31. Preeti D., Shubha E. A. & K. Singh, Computer Aided design and realization of wide band ultra low side lobe level antenna with mutual coupling compensated antenna elements', Proc. IEEE-APS, June 2007, pp 1397–1400, USA.
32. A. K. Singh, Shubha E. A. & Pramod Kumar, Design and Development of Semi Active Multi Beam Antenna for 3-D Surveillance Radar,' IRSI-2007, India
33. A. K. Singh, Shubha E. A. & Pramod Kumar, Multi Beam

Antenna System for portable 3-D Surveillance Radar, Proc EuCAP- 2007, UK
34. Preeti D., Shubha E. A. & A. K. Singh, A computer aided approach for designing very low side lobe triplate dipole array for multi beam antenna system, Proc IEEE – ISM06, pp. 349–357, Dec 2006, India
35. A. K. Singh, Shubha E. A. & Pramod Kumar, CAD of electronically steerable slotted waveguide array antenna for airborne active aperture radar, Proc IEEE – ISM06, pp. 418–423, Dec 2006, India
36. P. Srinivas, A. K. Singh, Y. Mohan Rao & S. Christipher, Design of MMIC based Electronically Steerable RF Multi Beam Former for 3-D Radars, Proc. IEEE-MTT-S 2005, p. 391–394, USA
37. Shubha Elizabeth, A. K. Singh, Y. Mohan Rao & S. Christopher, Tunable Compact Feeder Network for Shaped Beam Antennas of Long Range 3D Surveillance Radar, Proc. Progress in Electromagnetic Research Symposium (PIERS-2005), China
38. Anil K. Singh, Design of a Modified Blass Matrix for Multiple Beam Antenna, Proc. International Conference on Microwaves, Antennas, Propagation and Remote Sensing (ICMARS-04), 23–25 November 2004, Jodhpur, India
39. Hansen R. C., Phased Array Antennas, New York, John Wiley, 1998
40. Shenoy R. P., Phased Array Antennas, Advanced Radar Techniques and Systems, G Galati, Peter Peregrinus, 1993, Chapt 10
41. Brookner Eli, Phased Array and Radars — Past, present and future, Microwave J., No. 1, 2008, pp. 24–46
42. S. K. Kaul & B. Bhat, Microwave and millimeter wave phase shifters, Artech House, Boston, 1991

Dr. A. K. Singh obtained his Ph.D. in 1991 in electronics engineering from Banaras Hindu University, Varanasi (INDIA). He joined Electronics & Radar Development Establishment (LRDE), Bangalore in November 1991 and presently heading the R&D group involved in the design & development of 3D Low Level Active Aperture Radar and Antenna / Array Antenna systems for various radar applications which includes medium range / long range 3D / 4D radar systems, airborne fire control radar, maritime patrol radar, SAR for UAVs and antenna systems for LIC radars.

As a Project Director of 3D radar ASLESHA for Indian Air Force, he led the team towards successful development, qualification, extensive user field trials, user acceptance and production of the fully engineered & deployable 3D Low Level Light Weight Semi distributed Active Aperture Radar (ASLESHA) for mountainous terrains & high altitude operations. Apart from leading the project, he was the core designer responsible for conceptualizing the ASLESHA radar architecture and sub-system configuration and establishing semi-distributed active aperture antenna design and calibration process in LRDE.

As a Chief designer and project manager he has established Multi Beam Antenna (MBA) Technology in the country, thereby enabled the development and qualification of antenna systems for 3D Surveillance Radar Rohini for IAF, Revathi for Indian Navy and Tactical Control Radar for Indian Army). He was instrumental in qualifying the antenna, completing the TOT, streamlining the production of indigenous antenna system at M/s Bharat Electronics (BEL) concurrently.

As a core designer & project manager, he is responsible for establishing a comprehensive Design, analysis and manufacturing technologies for developing high performance slotted waveguide array antennas. He has been responsible for developing, qualifying and supplying more than 20 nos. of high performance X-band slotted waveguide array antenna for Multi Mode Radar to M/s ADA to meet the limited series production requirements of LCA. This fully qualified & certified (by RCMA/DGAQA) antenna is part of the Multi Mode Radar being developed for LCA program. He is also responsible for developing & exporting 10 Nos. of Slotted Waveguide Array Antennas to M/s PIT, Poland in last two years and generated considerable revenue to the organization.

He has also developed various other antenna and feed systems like corrugated feed for Akash command guidance array, VSAT antenna feeds (more than 200 of which has been delivered to ITI) and High power dual polarised feeds (in S-band & C-band) for Doppler Weather Radar developed by ISRO.

He has served as a chairman of technical program committee of International Radar Symposium (India) (IRSI-2007), Co-chairman, technical program committee of IEEE International Symposium on Microwaves in 2008, International correspondent & member of IEEE Radar conference (France) in 2009 and member of various other international & National conferences. He has authored more than 90 research papers in different international / national journals and symposiums. He has 3 copyrights and 3 patents to his credit. For his novel invention and significant contributions, he has been awarded NRDC (National Research Development Corporation) meritorious invention award in 1997, DRDO National Science Day commendation in 2005, DRDO Technology Group Award in 2006, DRDO performance excellence award in 2008 and IETE-IRSI award in 2009. He is member of society of electronics engineers and a Fellow of IETE.